Functional Characterization of p.Ser420Phe CRY2 Variant

by

Gizem Çağla Parlak

A Dissertation Submitted to the
Graduate School of Sciences and Engineering
in Partial Fulfillment of the Requirements for
the Degree of

Master of Science

in

Molecular Biology and Genetics

KOÇ
ÜNİVERSİTESİ

June, 2023

Functional Characterization of p.Ser420Phe CRY2 Variant

Koç University

Graduate School of Sciences and Engineering

This is to certify that I have examined this copy of a master's thesis by

Gizem Çağla Parlak

and have found that it is complete and satisfactory in all respects,
and that any and all revisions required by the final
examining committee have been made.

Committee Members:

Prof. İ. Halil Kavaklı

Prof. Mahmut Çalışkan

Asst. Prof. Onur Öztaş

Date: 20.06.2023

This thesis is dedicated to my family.

ABSTRACT

Functional Characterization of p.Ser420Phe CRY2 Variant

Gizem Çağla Parlak

Master of Science in Molecular Biology and Genetics

June, 2023

The circadian clock is an innate mechanism that enables organisms to adapt to the rhythmic changes of the environment. In mammalian cells, this mechanism is achieved by the interaction of four core clock proteins (CRYs, PERs, CLOCK, and BMAL1). Human clock-gene variations are associated with numerous behavioral and physiological diseases, such as sleep, metabolism, addiction, neurological disorders, and endocrine and metabolic. However, little is known about the possible effects of variations at the molecular level. Currently, the functional consequence of these variations and the strength of their association with the disease remains unclear. The functional analyses of variants help us to understand the role of amino acid residues in the structure and function of proteins.

In this study, rare CRY2 variants were selected from the 1000 Genomes Project, and the Ensembl database. SNPs were filtered based on the prediction of pathogenicity using *in silico* tools. Using the 3D structure of the CRY2 protein, the variant (p.Ser420Phe CRY2) located in the vicinity of the coiled-coil-like helix (CC helix) was functionally characterized.

We have found that the p.Ser420Phe CRY2 had reduced repression activity on CLOCK/BMAL1-driven transcription and showed rescued circadian rhythm with a shorter period than wild type in *Cry1*$^{-/-}$*Cry2*$^{-/-}$ double knockout mouse embryonic fibroblast cell line. Moreover, the variant had reduced affinity to other core clock proteins CLOCK and PER2 and could not properly localize in the nucleus using biochemical methods. Further stability results suggested that the p.Ser420Phe CRY2 variant was degraded by a noncanonical mechanism.

Collectively, our results show that the CC helix region plays an important role in the degradation of CRY2, interaction with other core clock proteins, also nuclear shuttling.

ÖZETÇE

p.Ser420Phe CRY2 Varyantının İşlevsel Karakterizasyonu

Gizem Çağla Parlak

Moleküler Biyoloji ve Genetik, Yüksek Lisans

Haziran, 2023

Sirkadiyen saat, organizmaların çevrenin ritmik değişikliklerine uyum sağlamasını sağlayan doğuştan gelen bir mekanizmadır. Memeli hücrelerinde bu mekanizma, dört çekirdek saat proteininin (CRY'lar, PER'ler, CLOCK ve BMAL1) etkileşimi ile sağlanır. İnsan saat geni varyasyonları, uyku, metabolizma, bağımlılık, nörolojik bozukluklar ve endokrin ve metabolik gibi çok sayıda davranışsal ve fizyolojik hastalık ile ilişkilidir. Ancak moleküler seviyedeki varyasyonların olası etkileri hakkında çok az şey bilinmektedir, bu varyasyonların fonksiyonel sonuçları ve hastalıkla olan ilişkileri belirsizliğini korumaktadır. Bununla birlikte, varyantların fonksiyonel analizleri, proteinlerin yapısı ve işlevindeki rolünü anlamamıza yardımcı olur.

Bu çalışmada 1000 Genom Projesinden ve Ensembl veri tabanından nadir CRY2 varyantları belirlendi. Varyantlar, *silikonda* araçlar kullanılarak patojenite tahminine dayalı olarak seçildi. CRY2 proteininin 3 boyutlu yapısı kullanılarak, alfa heliks yakınında bulunan varyant (p.Ser420Phe CRY2) fonksiyonel olarak karakterize edildi.

p.Ser420Phe CRY2'nin CLOCK/BMAL1 güdümlü transkripsiyonda baskılama aktivitesini azalttığını ve *Cry1*$^{-/-}$*Cry2*$^{-/-}$ fare embriyonik fibroblast hücrelerinde vahşi tipten daha kısa bir süre ile kurtarılmış sirkadiyen ritim gösterdiğini bulduk. Ayrıca varyantın, diğer çekirdek saat proteinleri CLOCK ve PER2'ye afinitesinin azaldığını ve hücre çekirdeğine uygun şekilde lokalize edemediğini biyokimyasal çalışmalarımızla gösterdik. Dahası, stabilite deneyi sonuçları, p.Ser420Phe CRY2 varyantının kanonik olmayan bir mekanizma tarafından bozulduğunu gösterdi.

Toplu olarak, sonuçlarımız alfa heliks bölgesinin CRY2'nin bozulmasında, diğer çekirdek saat proteinleri ile bağlanmasında ve ayrıca hücre çekirdeği lokalizasyonunda önemli bir rol oynadığını göstermektedir.

AKNOWLEDGEMENTS

First, I would like to thank Prof. Halik Kavaklı for teaching me scientific thinking, sharing his knowledge, giving me a different perspective, and guiding me at every step. I would like to thank my committee members Prof. Mahmut Çalışkan and Asst. Prof. Onur Öztaş, for sharing their time and insightful comments about my research. Also, a special thanks to Asst. Prof. Şeref Gül for all his guidance from theory to the practice of experiments and for being a respectful teacher.

I was lucky to know a lot of brilliant scientists and great people during my time in the lab. Melis Çelik, thank you for being a super enthusiastic teacher, kind, and thoughtful person. Thanks to Zeynep Melis Gül, not just for teaching me fractionation but also for being an understanding and super cool friend; I can't wait to spend time with you in Switzerland. Barış Çakılkaya, life in the lab is not the same without you; you can be a superhero for making me laugh so hard even under stressful conditions. Bahar Çamur and Şafak Işın, you are out of sight but not out of mind. I thank you both not just for the thing that you taught me in the lab but also for the good memories that I always remember with a smile. Thanks to Begüm Baybalı for the talks that we had about the boys, even though the reporters think that we talked about super important science stuff. Saliha Sürme, if you weren't in the lab after Barış graduated, I could never laugh in the lab; your confidence and uniqueness are truly inspiring. Speaking about inspiration, Başak Velioğlu, your courage of not being afraid to show who you are really had an impact on me. Also, if there weren't for you, I could never learn French. Onur Özcan, I would like to thank you not just for the colorful images that you do on your computer but sharing all your knowledge with everyone around you. You saved me from reading tons of papers, you are the invisible hero of our lives. Special thanks to Selahattin Aydoğan, not just for your help with this thesis but also for making me smile. It is hard to be kind and funny at the same, but you do it so effortlessly; anyone who is working with you is lucky to have you in their lives.

I thank the most to my parents. If there weren't you, forget about this thesis, I couldn't accomplish anything. Thank you for your endless support. Everything I will achieve in my whole life will be because of you. Speaking of support, Kadir Oğulcan Palabıyık, you are the lemon of my cocktail, the chocolate topping of my forest fruit ice cream. I wouldn't be the same person without your love and support. Thank you for that.

Finally, I thank TUBITAK-KBAG 121Z862 for the financial support of this project.

TABLE OF CONTENTS

LIST OF TABLES

LIST OF FIGURES

ABBREVIATIONS

ADHD	Attention Deficit Hyperactivity Disorder
AMPK	Adenosine Monophosphate-Activated Protein Kinase
BHLH	Basic Helix-Loop-Helix
BMAL1	Aryl Hydrocarbon Receptor Nuclear Translocator-Like Protein 1
CC	Coiled Coil
CCG	Clock-controlled Gene
CHX	Cycloheximide
CK	Casein Kinase
CLOCK	Circadian Locomotor Output Cycles Caput
Co-IP	Complex Immunoprecipitation
CPF	Cryptochrome/Photolyase Family
CRY	Cryptochrome
DBP	D-Box Binding Protein
DMEM	Dulbecco's Modified Eagle's Medium
DXM	Dexamethasone
ECL	Enhanced Chemiluminescence
EDTA	Ethylenediaminetetraacetic Acid
FAD	Flavin Adenine Dinucleotide
FASP	Familial Advanced Sleep Phase
FBXL	F-Box and Leucine-Rich Repeat Protein
FBXW	F-Box And WD Repeat Domain
HEK 293T	Human Embryonic Kidney
HEPES	N-2-hydroxyethyl Piperazine-n'-2-ethane Sulfonic Acid
HRP	Horseradish Peroxidase
ipRGC	intrinsically photosensitive Retinal Ganglion Cells
LRR	Leucine-rich Repeat
LUC	Luciferase
MEF	Mouse Embryonic Fibroblast
NFIL	Nuclear Factor Interleukin
NLS	Nuclear Localization Signal
PAS	PER-ARNT-SIM
PBS	Phosphate-buffered Saline

PCR	Polymerase Chain Reaction
PDD	Persistent Depressive Disorder
PEI	Polyethyleneimine
PER	Period
PHR	Photolyase Homology Region
PLB	Passive Lysis Buffer
PIC	Protease Inhibitor Cocktail
PVDF	Polyvinylidene Fluoride
ROR	Retinoic Acid-Related Orphan Nuclear Receptor
RRE	ROR-Enhancer Element
SAD	Seasonal Affective Disorder
SCN	Suprachiasmatic nucleus
SNP	Single Nucleotide Polymorphism
TBS	Tris-buffered saline
TrCP	Transducin repeat Containing Protein
TTFL	Transcriptional/Translational Feedback Loop
WT	Wild Type

Chapter 1:
INTRODUCTION

Almost all organisms, from single-celled bacteria to advanced multicellular humans, have endogenous biological cycles to create homeostasis and enhance survival in response to environmental disturbances. The circadian rhythm is the endogenous oscillator that controls behavior and physiology in relation to daily cycles like the day-night cycle (Dunlap et al., 2004).

Transcriptional/translational feedback loops (TTFLs) regulate the rhythm at the molecular level. The primary TTFL is made up of core clock genes: clock, bmal1, pers, and crys. The CLOCK-BMAL1 complex operates as the loop's positive transcriptional element, whereas CRY and PER proteins act as negative. CLOCK-BMAL1 binds to the E-box of multiple oscillating clock genes and enhances their expression, including cry and per. When their levels rise in the cytoplasm, they translocate to the nucleus, interacting with the CLOCK-BMAL1 complex and suppressing their own expression (Takahashi, 2017). Then, PER and CRY are destroyed by beta-TrCP1 and FBXLs, respectively, so the clock gene expression resumes (Reischl et al., 2007; Siepka et al., 2007).

CRYs are essential for the functional clock mechanism. It is reported that CRY variations have been linked to various illnesses, including sleep problems, diabetes, and psychiatric disorders. However, the functional consequence of these variations and the strength of their association with the diseases remains unclear. Therefore, in this study, rare human CRY2 single nucleotide polymorphisms (SNPs) are selected from the 1000 Genomes Project and Ensembl database. Based on their pathogenic probability, the SNPs that are potentially disease-causing are determined by various *in silico* tools, including SIFT, PolyPhen, CADD, REVEL, MetaLR, MutationAssessor, and MutationTaster. These potentially disease-causing SNPs are mapped to see whether they are located in functionally important regions of CRY2.

CRY2 has two main domains, which are the PHR domain at the N terminal, which is crucial to maintain rhythmicity and a variable C terminal tail required for the amplitude of the rhythm (Khan et al., 2012; Gao et al., 2013). The PHR domain contains a FAD-binding pocket, a secondary pocket, and a coiled-coil-like helix (CC helix). The

secondary pocket is shown to be essential for the adequate localization of the CRY2 into the nucleus and for maintaining circadian rhythm (Parlak et al., 2022). CC helix of CRYs interacts with the C-terminal of PER2. (Ozber et al., 2010; Nangle et al., 2014. Moreover, FBXL3 and FBXL21 are the main ubiquitin ligases responsible for CRY degradation and compete with PER2 around this region for CRY binding; therefore, this region is also important for the stability (Hirano et al., 2013 Yoo et al., 2013; Schmalen et al., 2014)). Moreover, deleting the CC helix and nuclear localization signals (NLS) on CRY tails causes exclusive cytosolic localization; thus, the CC helix is also essential for proper nuclear shuttling. For these reasons, I conducted functional analyses of CRY2 SNP in the vicinity of the CC helix to understand the role of amino acid residues in the structure and function of proteins.

To gain insight into the functional role of this region, in this study, the repression activity of CRY2 SNP on CLOCK/BMAL1-driven transcription was investigated with *Per1-dLuc* repression assay, and the SNP showed reduced repressor activity. Furthermore, since this region is important for PER2 and FBXLs binding, protein complex immunoprecipitation was performed, and observed that the SNP had reduced affinity to PER2, as well as CLOCK. Also, the affinity of SNP to both FBXL3 and FBXL21 was destroyed. Additionally, due to the importance of this region on nuclear shuttling, the subcellular fractionation was performed, and observed that the SNP had reduced levels on the nucleus and the cytosol, which implies that the SNP might have reduced stability. Since its key location for FBXL binding and lower expression in both cytosol and nucleus, the effect of CRY2 SNP on CRY degradation was investigated in detail with CHX chase experiments. It is observed that the SNP had significantly reduced half-life. To investigate how its stability was regulated, the CHX chase experiment was repeated with MG132 treatment, used to inhibit protease and the SNP was still unstable, suggesting that it was degraded by a noncanonical mechanism. CRY1 is degraded by lysosome in mice with obesity-associated hyperglycemia (Toledo et al., 2018). Therefore, the lysosomal degradation was investigated as an alternative by performing a CHX chase experiment with lysosome inhibitors PepstatinA and E64-d, and the stability of the SNP increased, indicating that the lysosome regulates its stability. Finally, it is tested if the SNP rescue the circadian rhythm in *Cry1*$^{-/-}$*Cry2*$^{-/-}$ double knockout mouse embryonic fibroblast cell line under endogenous conditions, and the SNP showed a rhythm with a shorter period which is in line with its reduced repression activity.

The effect of the SNP at the vicinity of the CC helix of CRY2 on the molecular clockwork was studied to gain more knowledge about the role of the CC helix. Collectively, this region is crucial for the degradation, interaction with PER2, CLOCK, FBXL3, and FBXL21, nuclear shuttling, and thus the repression activity.

Chapter 2 of the thesis provides a detailed literature review of circadian rhythm, focusing on the mammalian molecular mechanism with the role of CRY2 on the mechanism and the structure of CRY2.

Chapter 3 of the thesis describes the materials and methods used in this research.

Chapter 4 of the thesis shows the results of this research.

Finally, the results are discussed in Chapter 5 of the thesis, followed by concluding remarks.

Chapter 2:

LITERATURE REVIEW

2.1 Overview of Biological Rhythms

The Earth's location and rotation around the sun and moon create daily temperature, humidity, light variations, and changes in the season and the length of day and night throughout the year. Almost all species, from single-celled bacteria to complex multicellular humans, have endogenous biological rhythms to establish homeostasis and promote survival in response to these environmental changes (Dunlap et al., 2004). These rhythms are categorized as infradian, ultradian, and circadian rhythms based on the length of their period. Infradian rhythms govern the events occurring longer than a 24-hour period, which includes migration, hibernation, menstruation, and reproductive behaviors (Goldman, 2001; Rutovskaya et al., 2020). On the other hand, ultradian rhythms include breathing, feeding, hearth beat, and urination, occurring in less than 24-hour cycles (Aschoff, 1981). Circadian rhythms are the behavioral and physiological changes that occur every 24 hours, including the sleep-wake cycle and circulation of hormones, such as melatonin and cortisol (Dunlap et al., 2004). Among these biological rhythms, the circadian rhythm attracts most of the attention from researchers because of its connection to nearly all of the physiological and metabolic processes.

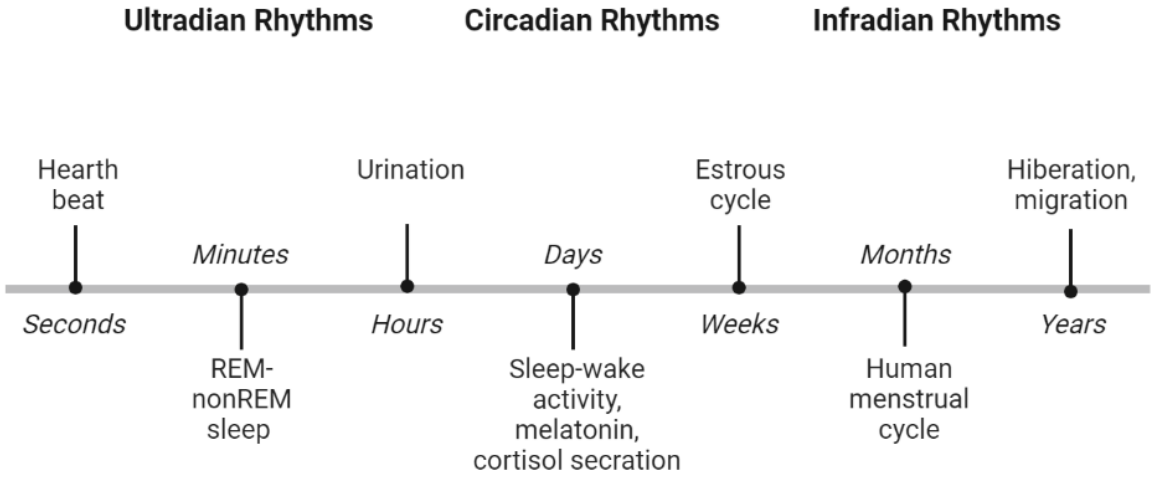

Figure 2.1. Schematic representation of the rhythms. Examples of ultradian, circadian, and infradian rhythms are depicted.

2.2. Circadian Rhythms and Clocks

The circadian rhythm is the internal timing system of organisms that allows them to adapt to daily periodic environmental changes, the most notable of which is the Earth's day and night cycle, by altering their physiological and behavioral activities. These physiological and behavioral changes are represented as rhythms with mathematical properties: period, amplitude, and phase (Vitaterna et al., 2001). The period is the time passed between the waves' two peaks. The amplitude is the distance between the highest and lowest points of the waves (Vitaterna et al., 2001). Moreover, the phase is the timing of a selected point on a wave concerning an external time point called "Zeitgeber," which are environmental clock-resetting changes including light, temperature, and food (Vitaterna et al., 2001; Saini et al., 2019).

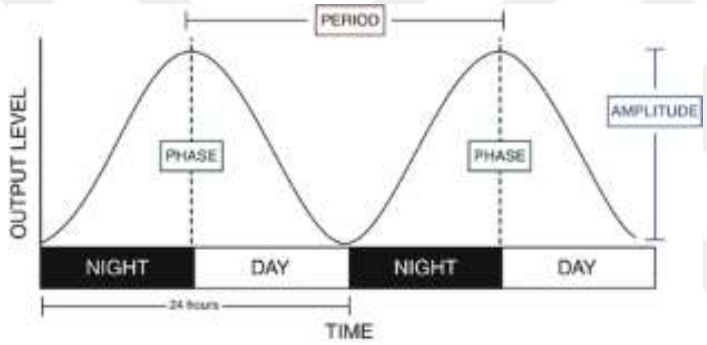

Figure 2.2. Properties of the circadian rhythm. The period, amplitude and phase of the rhythm is depicted. This figure is adapted from Evans & Silver 2022 with permission found in Appendix.

The discovery of the circadian rhythm dates to the 1700s. In 1729, Jean-Jacques d'Ortus de Mairan designed a simple experiment in which he observed *Mimosa pudica* under constant darkness and observed its behavior. He observed that Mimosa pudica leaves open in the daytime and close at night time, even under constant darkness, indicating that the plant has an internal clock (Dunlap et al., 2004; Klarsfeld et al., 2013). The scientist interpreted this observation as the plant senses the sunlight even if it is not exposed to it. In 1832, Augustin Pyramus de Candolle proposed the concept of an endogenous internal clock. He observed the *Mimosa pudica* under constant light and observed that the opening and closing of the leaves happens in 22-hour intervals, not 24 as the Earth's rotation around the sun, so he proposed that the plant should have an internal clock responsible for this 22-hour rhythmicity (Wang, 2018). After these initial studies, the research in the field of the circadian clock expanded. In the 1970s,

Pittendrigh and Aschoff pioneered these studies. They developed the concept of Zeitgeber, which means ‘’time giver’’. They drove that the rhythmic day-night changes in the organism’s behavior and physiological activities take place even under constant conditions, like Mairan and Candolle was also observed, thanks to an internal pacemaker with the periods deviating from 24 hours. However, the circadian rhythms were entrained to a 24-hour daily cycle due to environmental factors, and this was defined as Zeitgeber (Aschoff et al., 1978; Pittendrigh, 1981). Moreover, Aschoff observed some patterns in several animal species named ‘’Aschoff’s rules’’. These rules include observation of the periods of diurnal and nocturnal mammals under constant light and dark. Such as, light increases the activity of diurnal animals but decreases the activity of nocturnal animals. Moreover, at a low light intensity, nocturnal animals lose their circadian rhythmicity but not diurnal animals; this shows that the circadian pace is regulated by light intensity (Aschoff, 1979).

Even though Aschoff’s research provided insights into the internal pacemaker, the molecular mechanism was still unknown. In 1971, the first molecular component of the circadian rhythm was discovered by Konopka and Benzer. They made genetic screening on *D. melanogaster* and three mutants that showed significantly different periods than 24 hours of the rhythm. They found that all these three mutants located on the same gene on the X chromosome, called this gene *Period* (Konopka & Benzer, 1971). Around the same time, it was discovered that suprachiasmatic nucleus (SCN) lessons cause the loss of the circadian rhythm in mice (Moore et al., 1972). This initial study paved the way for other studies on the SCN and circadian rhythm. SCN is located in the brain’s hypothalamus and is composed of nearly 10000 neurons and functions as the pacemaker. Later, other genes that play critical roles in the molecular architecture of the circadian rhythm were discovered. In 1994, Takahashi’s group found the circadian locomotor output cycles kaput (*Clock*) gene by genetic screening mutant mice with malfunctioning clocks (Vitaterna et al., 1994). Two years later, CRYPTOCHROME (CRY) was later founded by Aziz Sancar and his colleagues (Hsu et al., 1996). Also, in 1997, Hogenesch and his colleagues discovered the last essential molecular component of the mammalian circadian clock, Brain and muscle Arntl-1 like (BMAL1) (Hogenesch et al., 1997).

Another ground-breaking discovery in the field was that in peripheral mouse tissues such as the liver, kidney, and lung, oscillations of core-clock gene *period* was discovered. The fascinating thing was the oscillation of *period* happens with different

phase than the oscillations of the same gene in SCN, which indicates that the peripheral tissues have their own clock and this is called peripheral clock (Balsalobre et al., 1998). SCN acts as a master clock; it receives light input from the environment by intrinsically photosensitive retinal ganglion cells (ipRGC) (Kavakli & Sancar, 2002). SCN is stimulated due to the light signal and synchronizes the peripheral clocks by neural and hormonal signals (Dibner et al., 2010). An organism's physiological and behavioral responses are regulated as an output, such as the sleep-wake cycle, metabolism, body temperature, hormone secretion, and glucose-lipid metabolism (Feng et al., 2012).

2.3. Molecular Architecture of Mammalian Circadian Rhythm

At the molecular level, the circadian rhythm operates by three conserved intracellular transcriptional/translational feedback loops (TTFLs) (Ko& Takahashi, 2006). The first loop is driven by four core clock proteins: CLOCK (Circadian Locomotor Output Cycle Kaput), BMAL1 (Brain and Muscle Aryl Hydrocarbon Receptor Nuclear Translocator (ARNT)-like protein 1), CRYPTOCHROME (CRY1, CRY2), and PERIOD (PER1, PER2, PER3) (Takahashi, 2017). CLOCK-BMAL1 complex functions as a positive transcriptional element. CLOCK and BMAL1 bind each other's basic helix-loop-helix (bHLH) and PER-ARNT-SIM (PAS) domains and heterodimerizes (Huang et al., 2012). CLOCK-BMAL1 complex bind to the E box of rhythmic genes through their bHLH domain. These rhythmically expressed genes are called clock-controlled genes (CCGs): *Dbp*, *Rev-erb α/ß,* as well as *Pers* and *Crys*. *Pers* and *Crys* act as negative arms of this TTFL. After they are expressed in the nucleus, they translocate to the cytoplasm, where they are translated (Takahashi, 2017). In the cytoplasm, the PER and CRY proteins interact with each other as well as with the serine/threonine kinases casein kinase 1δ (CK1δ) and CK1ε and translocate back into the nucleus as complex, where they interact with CLOCK–BMAL1. CK1δ phosphorylates CLOCK, leading to the release of the complex from the E-box (Takahashi, 2017; Cao et al., 2021). Consequently, PER and CRY's own transcription is repressed, so as other CCGs'. When PER and CRY are degraded by ß-transducin repeat-containing protein 1 (beta-TrCP1) and F-Box and Leucine-Rich Repeat Proteins (FBXLs), respectively, the expression of CCGs starts again, and the loop continues (Reischl et al., 2007; Siepka et al., 2007).

The second TTFL regulates the expression of one of the core clock genes: *Bmal1*. The expression of *Bmal1* is controlled by the binding of retinoic acid-related orphan nuclear receptor (ROR) and REV-ERB proteins to the ROR enhancer elements (RREs)

in the promoter region of *Bmal1*. ROR binding enhances the *Bmal1* expression; on the other hand, binding of REV-ERB, whose expression is controlled by CLOCK–BMAL1 transactivation, competes with RORs to the RREs and repress *Bmal1* expression (Mohawk et al., 2012; Koike et al., 2012).

The third of these interlocking TTFLs is about the regulation of D-box binding protein (DBP) and nuclear factor interleukin 3 (NFIL3). DBP expression is under the control of CLOCK-BMAL1. NFIL3 expression is regulated by ROR and REV-ERB proteins. Like the regulation of BMAL1, ROR, and REV-ERB competes for binding RREs in the promoter region of *Nfil3*. DBP binds to the D-box of some rhythmic genes and enhances their expression, including *Rors*, *Rev-erbs*, and *Pers*. Contrarily, NFIL3 competes with DBP to repress the expression of *Rors*, *Rev-erbs*, and *Pers* (Ripperger & Schibler, 2006; Takahashi, 2017).

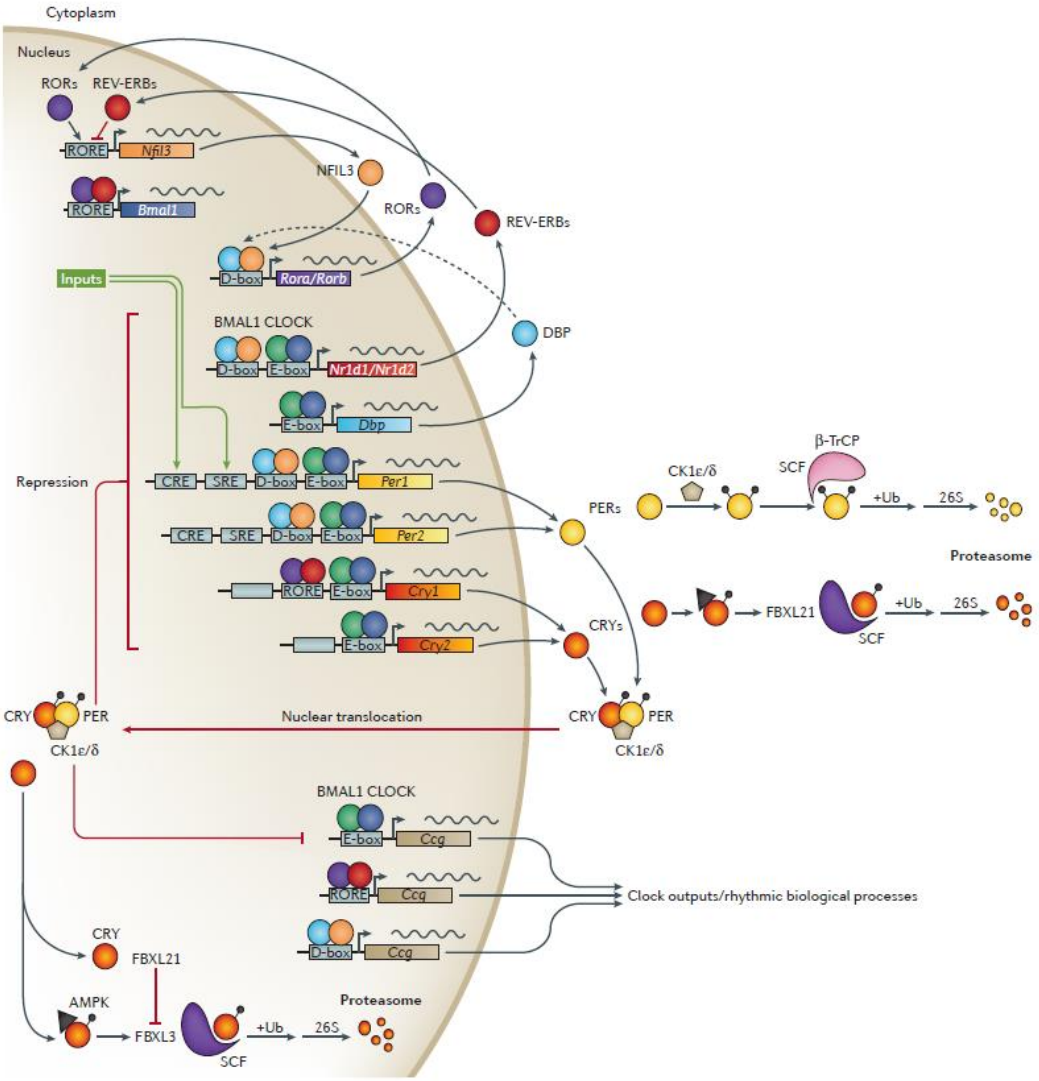

Figure 2.3. Visualization of mammalian circadian gene network. Three interconnecting TFFLs are displayed in detail. This figure is adapted from Takahashi, 2017 with permission found in Appendix.

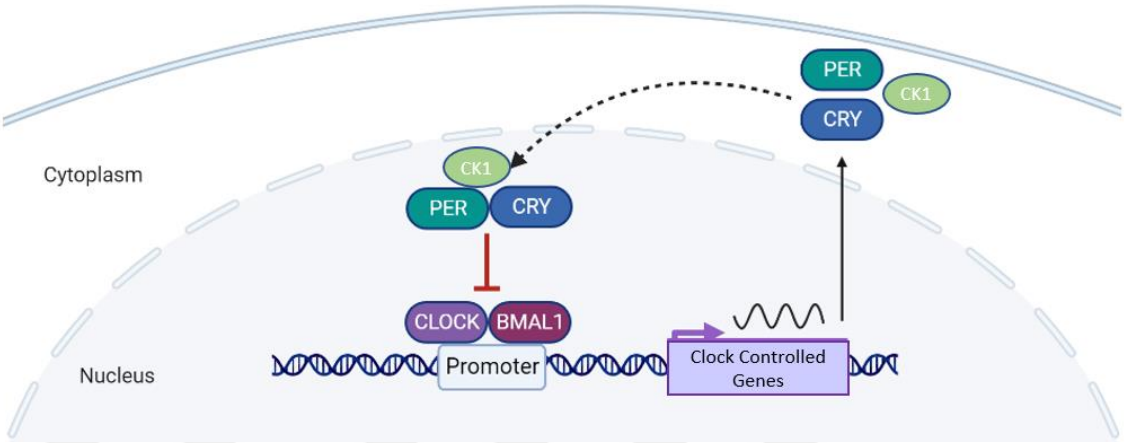

Figure 2.4. Visualization of primary TTFL of the mammalian molecular clockwork. The primary TTFL of mammalian circadian clock is displayed in detail.

2.4. Structure of CRYs

Cryptochromes are members of the photolyase/cryptochrome (PHR/CRY) family, a large group of proteins with similar structures but various functions (Öztürk et al., 2016). Cryptochromes comprise a conserved photolyase homology region (PHR) at the N terminal and a variable C terminal tail. The PHR domain is crucial to maintain rhythmicity, and the C terminal tail is required for the amplitude of the rhythm (Khan et al., 2012; Gao et al., 2013). These two domains are connected by a flexible inter domain linker.

The PHR domain contains a primary FAD-binding pocket, a secondary pocket, and a coiled-coil-like helix (CC helix) near the C terminal tail (Rosensweig et al., 2018). The FAD-binding pocket is where cryptochromes bind to FAD; however, they do not perform any photochemical activities (Özgür & Sancar, 2003). Molecular docking and co-immunoprecipitation analysis show that the secondary pocket of CRYs interacts with the CLOCK (Nangle et al., 2014). Moreover, this region is important for the nuclear localization of CRY2 and, in turn, its activity on CLOCK-BMAL1 transactivation (Parlak et al., 2022). Serine loop located close to the N-terminal, also play important roles in the CRY-PER2 interaction (Fribourgh et al., 2020; Ozcan et al., 2021). Moreover, CC helix of CRYs interacts with the C-terminal of PER2 (Ozber et al., 2010; Nangle et al., 2014). Additionally, the crystal structure reveals that the leucine-rich repeat (LRR) domain of

FBXL3 interacts with CRY2 at the same site as PER2; since FBXL3 and PER2 cannot interact with CRY2 at the same time without colliding, they compete for binding to CRY2 around the CC helix (Nangle et al., 2014). Furthermore, The 86% sequence identity and conservation of CRY binding residues between FBXL3 and FBXL21 suggest that FBXL21 also binds to the same region of CRY (Hirano et al., 2013; Yoo et al., 2013; Schmalen et al., 2014). CC helix also takes part in nuclear shuttling. CRY tails contain nuclear localization signals (NLS), the loss of which does not result in the exclusive localization of CRY1 to the cytoplasm; this is only accomplished by also deletion of the CC helix (Chaves et al., 2006).

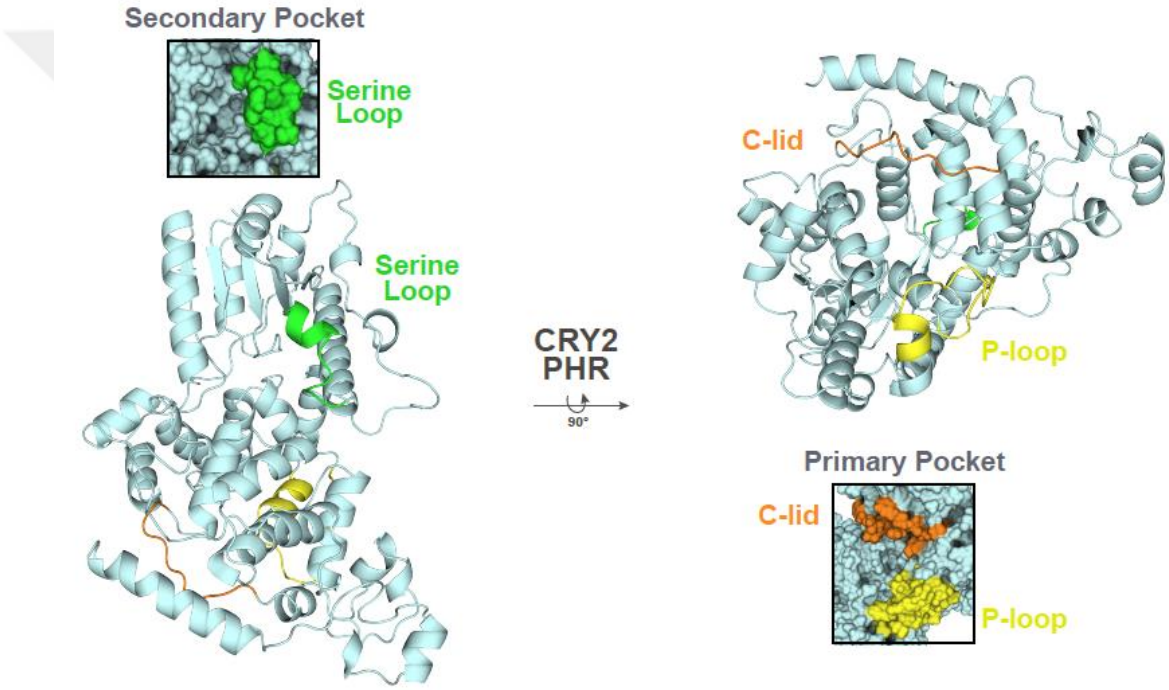

Figure 0.5. Visualization of the PHR domain on 3D Structure of mCRY2. The mCRY2 structure was shown as a ribbon diagram. The serine loop was colored green, the C-lid orange, and the P-loop yellow.

2.5. Degradation of CRYs

The degradation of core-clock proteins is crucial for regulating the feedback loops of the circadian clock mechanism (Hirano et al., 2016a). Kinases, phosphatases, and ubiquitin ligases are mainly responsible for the degradation (Hirano et al., 2016b). Arabidopsis CRY2 is regulated by first phosphorylation in a blue-light-dependent manner, which causes a conformational change in CRY2 that causes the recruitment of two distinct E3 ubiquitin ligases: $Cul4^{COP1/SPAs}$ and $Cul3^{LRBs}$ (Zuo et al., 2012; Chen et

al., 2021). In mammals, CRYs are ubiquitinated and degraded via multiple ubiquitin ligase complexes, including F-Box and leucine-rich repeat protein 3 (FBXL3) and F-box and leucine-rich repeat protein 21 (FBXL21). FBXL3 is predominantly localized in the nucleus and FBXL21 in the cytosol, with a slower degradation rate than FBXL3 (Busino et al., 2007; Hirano et al., 2013). Moreover, F-Box And WD Repeat Domain Containing 7 (FBXW7) is more recently discovered ubiquitin ligase is recruited to induce CRY2 degradation in trophoblast (Wu et al., 2021). Further, CRY1 is phosphorylated and destabilized by adenosine monophosphate–activated protein kinase (AMPK) nutrient dependently in mouse fibroblast (Lamia et al., 2009). Later research reveals that CRY1 is also degraded by lysosome, and when this pathway is induced, it contributes to obesity-associated hyperglycaemia (Toledo et al., 2018).

2.6. Diseases Related to CRY Mutations

CRY mutations are associated with numerous diseases, including sleep disorders, diabetes, and mood disorders. For example, a CRY2 SNP, where alanine residue at position 260 is replaced with a threonine, is linked with Familial Advanced Sleep Phase (FASP) in a family (Hirano et al., 2016c). The SNP is located in the FAD domain. It makes CRY2 more accessible to FBXL3 by changing the conformation, which boosts the degradation of CRY2, causes a shorter period, and reduces the phase shift associated with the advanced phase behavior. This study reveals that CRY2 degradation by FBXL3 is important for adequately regulating human sleep-wake behavior. A CRY2 intronic variant rs11605924 is associated with type 2 diabetes (Liu et al., 2011). On the other hand, an exonic CRY1 variant rs8192440 is associated with cluster headache disorder (Fourier et al., 2021).

The deletion of CRY1 exon 11 is linked to delayed sleep phase disorder (DSPD), which is a common type of insomnia (Patke et al., 2017). This dominant variant increases the CLOCK-BMAL1 affinity and increases the circadian period length, as seen in insomnia patients. Moreover, CRY1 SNP *CRY1*Δ6 c.825+1G>A is segregated from attention deficit hyperactivity disorder (ADHD) and DSPD in the affected family (Onat et al., 2020). This SNP reduces the interaction between CRY1 and CLOCK-BMAL1 and causes arrhythmicity. The same study reveals that, besides insomnia, the deletion of exon 11 is also related to major depressive disorder and anxiety (Onat et al., 2020).

Two CRY2 SNPs (rs10838524 risk allele A, rs10838527 risk allele G, and rs3824872 risk allele A) are found to be segregated with winter depression in a Swedish

sample population (Lavebratt et al., 2010). In addition, four CRY2 SNPs (rs10838524, rs7121611, rs7945565, rs1401419) are a significant risk factor for PDD (persistent depressive disorder) (Kovanen et al., 2013). A recent study reveals that Cry2 SNP rs2292912 is significantly associated with dyslipidemia and, indirectly, diabetes in African American and Hispanic/Latino populations (Salazar et al., 2021). Further, transcriptional increases for variants in Cry, rs2287161 (in CRY1), rs184039278 (in CRY1), and rs10838524 (in CRY2), are associated with the seasonal affective disorder (SAD) that is a type of depression (Dhawka et al., 2022). These SNPs cause lower amplitudes and phase-shift in the circadian rhythm.

Chapter 3:
MATERIALS AND METHODS

3.1. Site Directed Mutagenesis (SDM)

Phusion polymerase-based quick-change mutagenesis was used to generate single nucleotide change on pcDNA-*Cry2*-Myc-His using the primers in ''Table 3.1.''. Each PCR reaction consisted of 1X HF Buffer, 200 µM dNTP mix, 0.3 µM forward and reverse primers, 50 ng of the template plasmid, and 0.02 unit/µl of Phusion Hot Start Flex DNA Polymerase (NEB, catalog no.: M0535S) in a 50 µl of the final volume. The PCR reaction was performed at 98ºC for 2 minutes, 98ºC for 45 seconds, 55ºC for 30 seconds, and 68ºC for 10 minutes, 22 cycles, and final elongation of 68 ºC for 2 minutes. Q5® high-fidelity DNA polymerase-based quick-change mutagenesis was used to generate single nucleotide change on pMU2-P(*CRY1*)-(intron 336)-*Cry2*. 1X Q5® Buffer Pack, 200 µM dNTP mix, 0.5 µM forward and reverse primers, 50 ng of the template plasmid, 1X Q5® High GC Enhancer, and 0.02 unit/µl (NEB, catalog no.: M0491S) were used in the PCR reaction in a 25 µl of the final volume. The PCR reaction was carried out at 98ºC for 2 minutes, 98ºC for 20 seconds, 72ºC for 30 seconds, and 72ºC for 4 minutes, 12 cycles followed by 98ºC for 20 seconds, 60ºC for 30 seconds, and 72ºC for 4 minutes, 18 cycles followed by 72ºC for 5 minutes final elongation. PCR product is cleaned with PCR clean-up kit (Macherey Nagel, catalog no.: 740609.50) using manufacturer instructions. In 0.8% agarose gel, PCR products of both pcDNA-*Cry2*-Myc-His and pMU2-P(*CRY1*)-(intron 336)-*Cry2* were visualized. The samples were digested with 1 unit of FastDigest DpnI enzyme (Thermo Scientific, catalog no.: FD1703) for 1 hour at 37ºC and then inactivated at 80ºC for 5 minutes. 5 µl of the PCR product was transformed to TOP10 E. coli competent cells. Colonies were cultured, and the plasmids were isolated with a Nucleospin Plasmid kit (Macherey Nagel, catalog no.: 740588.50) following manufacturer instructions. The mutations were confirmed by Capillary electrophoresis sequencing (Macrogen).

Table 3.1. Primer sequences for SDM of mCRY2

mCRY2_R28H-F	GGTGCACTGGTTCCACAAAGGACTACGG
mCRY2_28H-R	CCGTAGTCCTTTGTGGAACCAGTGCACC
mCRY2_P122L-F	GAATATGACTCTGAACTCTTTGGGAAAGAACGGG
mCRY2_P122L-R	CCCGTTCTTTCCCAAAGAGTTCAGAGTCATATTC
mCRY2_G161W-F	CAGAATCATCGAACTGAATTGGCAGAAACCACCCCTTACC
mCRY2_G161W-R	GGTAAGGGGTGGTTTCTGCCAATTCAGTTCGATGATTCTG
mCRY2_R274C-F	CTCAGCCCCTACCTGTGCTTTGGATGCCTC
mCRY2_R274C-R	GAGGCATCCAAAGCACAGGTAGGGGCTGAG
mCRY2_C277Y-F	CGCTTTGGATACCTCTCCTGCC
mCRY2_C277Y-R	GGCAGGAGAGGTATCCAAAGCG
mCRY2_S279T-F	CTTTGGATGCCTCACCTGCCGCCTCTTC
mCRY2_S279T-R	GAAGAGGCGGCAGGTGAGGCATCCAAAG
mCRY2_S279C-F	GCTTTGGATGCCTCTGCTGCCGCCTCTTCTAC
mCRY2_S279C-R	GTAGAAGAGGCGGCAGCAGAGGCATCCAAAGC
mCRY2_L282P-F	CTCTCCTGCCGCCCCTTCTACTACCG
mCRY2_L282P-R	CGGTAGTAGAAGGGGCGGCAGGAGAG
mCRY2_W357C-F	CAGGCTTCCCTTGCATTGACGCCATC
mCRY2_W357C-R	GATGGCGTCAATGCAAGGGAAGCCTG
mCRY2_G369V-F	CTGAGGCAGGAGGCCTGGATCCACCACC
mCRY2_G369V-R	GGTGGTGGATCCAGGCCTCCTGCCTCAG
mCRY2_V379M-F	CTGGCCCGGCACGCTATGGCCTGCTTCCTC
mCRY2_V379M-R	GAGGAAGCAGGCCATAGCGTGCCGGGCCAG
mCRY2_V379G-F	CCGGCACGCTGGGGCCTGCTTC
mCRY2_V379G-R	GAAGCAGGCCCCAGCGTGCCGG
mCRY2_D405H-F	GAGCTGCTCCTGCATGCCGATTTCAG
mCRY2_D405H-R	CTGAAATCGGCATGCAGGAGCAGCTC
mCRY2_S409I-F	GGATGCCGATTTCATTGTGAATGCAGGCAG
mCRY2_S409I-R	CTGCCTGCATTCACAATGAAATCGGCATCC
mCRY2_S419F-F	CTGGATGTGGCTGTTCTGCAGTGCTTTC
mCRY2_S419F-R	GAAAGCACTGCAGAACAGCCACATCCAG
mCRY2_R439H-F	GGCTTCGGCCGACATACAGACCCCAGTG
mCRY2_R439H-R	CACTGGGGTCTGTATGTCGGCCGAAGCC

3.2. Per1-dLuc Repression assay on CLOCK–BMAL1 driven transactivation

$4x10^4$ HEK293T cells were reverse transfected with 125 ng of pCMV-Sport6-*CLOCK*, 50 ng of pCMV-Sport6-*Bmal1*, 50 ng of pGL3-*mPer1*:dLuc marker, 5 ng pGL4-*Renilla*, 20 ng of pFLAG-CMV-*Per2*, and WT or variant pcDNA-*Cry2*-His-Myc plasmids utilizing the polyethyleneimine (PEI) (Polysciences; catalog no.: 23966-1) transfection reagent on a 96-well opaque plate. To equalize transfected plasmid concentration, empty pcDNA plasmid was also transfected. To evaluate the activity of CLOCK-BMAL1 transactivation without the repressor, pcDNA-His-Myc without *Cry* was transfected. In each separate experiment, reverse transfections were performed in at least three replicates for each condition. After the plates were incubated for 24 hours, the

expression of firefly luciferase and renilla luciferase was measured with the Fluoroskan Ascent FL microplate reader using the Dual-Glo Luciferase Assay System (Promega) according to the manufacturer's procedure.

3.3. Protein extraction from mammalian cells and Western Blot

In order to extract proteins, the cultured cells with 100% confluency were collected with ice-cold phosphate-buffered saline (PBS) (137 mM NaCl, 2.7 mM KCl, 10 mM Na2HPO4, 1.8 mM KH2PO4, pH 7.4). Then, they were centrifuged at 4000 g at 4ºC for 5 minutes. The pellet was lysed with ice-cold RIPA buffer (150 mM NaCl, 50 mM Tris, 0.1% SDS, 1% Triton-X, 1% protease inhibitor cocktail (PIC; catalog no.: 78430)), incubated 15 minutes on ice and centrifuged for 20 minutes at 15000 g at 4ºC. The supernatant was collected, and protein concentration was measured using Pierce 660nm Protein Assay Reagent (Thermo Scientific, catalog no.: XD341295) with an Epoch microplate reader at 660 nm. The lysates were then boiled for 10 minutes at 95ºC with 4X Laemmli Buffer (250 mM Tris-HCl at pH:6.8, 40% Glycerol, 4% SDS, 0.02% Bromophenol Blue, and 10% freshly added β-mercaptoethanol). The samples were run on SDS-PAGE and transferred to Polyvinylidene fluoride membrane (PVDF, Millipore, catalog no.: IEVH00005) by wet Western Blot transfer. The membrane was blocked with 5% milk solution 0.15% Tris-buffered saline (TBS)–Tween-20 for 1 hour and then incubated overnight at 4ºC on the shaker with the proper primary antibodies, washed with 0.15% TBS-T solution 3 times for 5 minutes, then incubated for 1 hour with the suitable secondary antibody at room temperature. The primary antibodies included Anti-FLAG (Sigma Aldrich, catalog no.: SLCJ3741), Anti-Myc (Abcam, catalog no.: ab18185), Anti-β-actin (Cell Signaling, catalog no.: 8H10D10), anti-Histone H3 antibody (Abcam; catalog no.: ab1791), monoclonal anti-α-tubulin antibody (Sigma–Aldrich; catalog no.: T9026), anti-SQSTM1 monoclonal antibody (Abnova, catalog no.: H00008878-M01), anti-Gal4(DBD) antibody (Santa Cruz, catalog no.: sc-577). HRP-conjugated anti-mouse (Santa Cruz; catalog no.: SC-358920), HRP-conjugated anti-rabbit (Cell Signaling; catalog no.: 7074) and rabbit polyclonal IgG antibody (Santa Cruz, catalog no.: sc-48805) were used as secondary antibodies. After the incubation with the secondary antibody, the membrane was again washed with 0.15% TBS-T solution 3 times for 5 minutes and visualized using fresh homemade ECL (1.25 mM luminol (Sigma, catalog no.: MKCP9100), 0.225 mM p-coumaric acid (Sigma, catalog no.: C9008-25G), 0.1 M Tris (pH = 8.8), H_2O_2 ($9x10^{-5}$ [v/v]) with BioRad ChemiDoc Touch.

3.4. Protein complex immunoprecipitation (Co-IP)

$4x10^5$ HEK293T cells per well were seed to 6-well plate. After 24 hours, when the cells reached 70% confluency, they were transfected with 500 ng WT or variant pcDNA-*Cry2*-His-Myc, 1000 ng Flag-CMV-*Bmal1*, 150 ng Flag-CMV-*CLOCK*, and 350 ng Flag-*PER2*-CMV using PEI. For determining the interaction with FBXLs, HEK293T cells were transfected with 500 ng WT or variant pcDNA-*Cry2*-His-Myc plasmids, 500 ng pBind-*FBXL3*-Gal4, and 500 ng pFLAG-CMV-*FBXL21*. After 24 hours, the cells were harvested with ice-cold PBS and centrifuged at 4000 g at 4°C for 5 minutes. The pellets were lysed in 300 µl passive lysis buffer (PLB) (15 mM HEPES, 5 mM NaF, 300 mM NaCl, 1% NP-40, and 1% freshly added PIC) and incubated for 15 minutes on ice. The samples were centrifuged for 20 minutes at 15000 g at 4°C; then, the supernatants were collected. 10% of the supernatant was saved as input. 10 µl EZview Red Anti-c-Myc Affinity Gel beads per sample (catalog no.: E6654) were equilibrated by washing twice with PLB. Supernatants and equilibrated resins were mixed for 2 hours at 4°C in a vertical rotator. After 2 hours, the samples were centrifuged for 30 s at 8200g at 4°C. Supernatants were removed, and beads were washed 3-times with PLB (without PIC). After the final centrifuge, the proteins from the beads were isolated by boiling in Laemmli Buffer, and Western blot was carried out as described in the ''Extraction of proteins from cells and Western Blot'' section.

3.5. Subcellular fractionation

$4x10^5$ HEK293T cells were seeded in a 6-well plate. After 24 hours, the cells were transfected with 500 ng WT or variant pcDNA-*Cry2*-His-Myc plasmids and 500 ng pFLAG-CMV-*PER2* by PEI. The cells were collected and lysed using cytosolic lysis buffer after 24 hours of incubation (10mM HEPES pH 7.9, 10mM KCl, 0.1mM EDTA, 0.05% NP40, proteasome inhibitor). Then samples were incubated for 15 minutes on ice and centrifuged for 5 minutes at 650 g at 4°C. The supernatant was saved as the cytosolic fraction, and the pellet was processed for the nuclear fraction. The nuclear fraction was washed twice with cytosolic lysis buffer and centrifuged for 5 minutes at 650 g at 4°C. The pellet was dissolved in nuclear lysis buffer (20 mM HEPES pH 7.9, 0.4 M NaCl, 1 mM EDTA, 10% glycerol, protease inhibitor), then sonicated (60% power, 10 seconds x 3 cycles) and centrifuged 15000 g for 5 minutes at 4°C, with the supernatant preserved as the nuclear fraction. The cytosolic fraction was also centrifuged at 15000 g for 5 minutes at 4°C, the cell debris was removed in the pellet, and the supernatant was preserved as the

cytosolic fraction. After determining the protein amount, the fractions were supplemented with Laemmli buffer, and Western blot was carried out as described in the ‘’Extraction of proteins from cells and Western Blot’’ section.

3.6. CHX Chase assays

A 12-well tissue culture plate was seeded with $2x10^5$ HEK293T cells per well. Using PEI, 500 ng WT or mutant pcDNA-*Cry2*-His-Myc plasmids and 500 ng pFLAG-CMV-*PER2* plasmids were transfected into the cells after they had attained 70% confluency. After 24 hours, cells were treated with 20 µg/ml cycloheximide (CHX; Sigma, catalog no.: 66819). The cells were collected in 4-hour intervals for 12 hours. Cells obtained immediately after CHX treatment were labeled as 0 h. Moreover, the cells are treated with CHX (20 µg/ml) plus 10 µM MG-132 (Sigma, catalog no.: 1211877-36-9) to examine the effect of proteasome inhibition. And to investigate the lysosomal inhibition, the cells were treated with CHX (20 µg/ml) and 5 µg/ml PepstainA (Sigma, catalog no.: P5318) combined with 5 µg/ml E64-d (Santa Cruz, catalog no.: sc201280A) -gifted by Prof. Dr. Devrim Gözüaçık, Koç University-. Protein amounts were detected using Western blot as described in the ‘’Extraction of proteins from cells and Western Blot section.

3.7. Real-Time bioluminescence rescue assay

$4x10^5$ MEF *Cry1*$^{-/-}$*Cry2*$^{-/-}$ cells (gifted by Prof Ueda, RIKEN, Japan) were seeded into 35 mm culture dishes. The cells were transfected with 4000 ng pGL3-*Per2*-dLuc (luciferase reporter), pMU2-P(*CRY1*)-(intron 336), and WT or variant pMU2-P(*CRY1*)-(intron 336)-*Cry2* using the FuGENE6 transfection reagent (Promega; catalog no.: E2691) after 24 hours, when they have reached 70% confluency. After 3 days of incubation, the cells were reset with 0.1 µM dexamethasone (DXM; Sigma Aldrich; catalog no.: D4902). 2 hours after resetting; the medium was replaced with lumicycle medium (10 g Dulbecco’s modified Eagle’s medium powder (Sigma; catalog no.: D-2902; 10× 1 l), 0.35 g sodium bicarbonate (tissue culture grade; Sigma; catalog no.: S5761), 3.5 g D(+) glucose powder (tissue culture grade; Sigma; catalog no.: G7021), 10 ml 1 M HEPES buffer (Gibco; catalog no.: 15140-122), 2.5 ml penicillin/ streptomycin (100 µg/ml), 50 ml 5% fetal bovine serum, and up to 1 l sterile Milli-Q water) with 0.1 µM freshly added luciferin. The plates were then sealed with silicone grease and placed in the LumiCycle 32 Luminometer (Actimetrics). The bioluminescence readings were recorded for 70 seconds every 10 minutes for 5 days.

Chapter 4:
RESULTS

4.1. Selection of CRY2 SNPs

Rare human CRY2 single nucleotide polymorphisms (SNPs) were identified from the 1000 Genomes Project and Ensembl database, and approximately 300 SNPs were identified. Using several *in silico* tools such as SIFT, PolyPhen, CADD, REVEL, MetaLR, and MutationAssessor, these SNPs were filtered out with pathogenic probability. These variants were classified as a "variant of uncertain significance" by the American College of Medical Genetics and Genomics guideline *(Table. 4.1.)*. MutationTaster predicted these variants as "disease-causing.". We previously characterized these mutations at the molecular and cellular level (Parlak et al., 2022).

Table 4.1. The clinical features of CRY2 SNPs

Position in CDS(NM_021117.4)	Position in protein(NM_021117.4)	ACMG	gnomAD	ClinVar
c.86G>A	p.Arg29His	VUS (PM2, PP3)	not detected	—
c.368C>T	p.Pro123Leu	VUS (PM2, PP3)	not detected	—
c.484G>T	p.Gly162Trp	VUS (PM2, PP3)	not detected	—
c.823C>T	p.Arg275Cys	VUS (PM2, PP3)	not detected	—
c.833G>A	p.Cys278Tyr	VUS (PM2, PP3)	not detected	—
c.838T>A	p.Ser280Thr	VUS (PM2, PP3)	not detected	—
c.839C>G	p.Ser280Cys	VUS (PM2, PP3)	not detected	—
c.848T>C	p.Leu283Pro	VUS (PM2, PP3)	not detected	—
c.1074G>C	p.Trp358Cys	VUS (PM2, PP3)	not detected	—
c.1138G>A	p.Val380Met	VUS (PM2, PP3)	f = 0.000003991	—
c.1139T>G	p.Val380Gly	VUS (PM2, PP3)	Not detected	—
c.1216G>C	p.Asp406His	VUS (PM2, PP3)	not detected	—
c.1229G>T	p.Ser410Ile	VUS (PM2, PP3)	not detected	—
c.1259C>T	p.Ser420Phe	VUS (PM2, PP3)	not detected	—
c.1319G>A	p.Arg440His	VUS (PM2, PP3)	f = 0.000003991	—

SNPs were located at the different regions of CRY2: p.Pro123Leu, p.Asp406His, and p.Ser410Ile variants at the rim of the secondary pocket; p.Arg29His, and p.Arg275Cys inside the secondary pocket; p.Cys278Tyr, p.Ser280Thr, p.Ser280Cys, and p.Leu283Pro at the back of the secondary pocket; p.Ser420Phe at the vicinity to CC helix; p.Trp358Cys, p.Val380Met, p.Val380Gly, and p.Arg440His at close to C-terminal lid *(Fig. 4.1.)*. Mutations located at the rim of the secondary pocket are shown to be important for the proper localization of the CRY2 into the nucleus and for maintaining circadian rhythm (Parlak et al., 2022). In this thesis, I performed a detailed characterization of the

p.Ser420Phe CRY variant *(Fig. 4.2.)*, located in the vicinity of CC helix, using different biochemical and molecular tools.

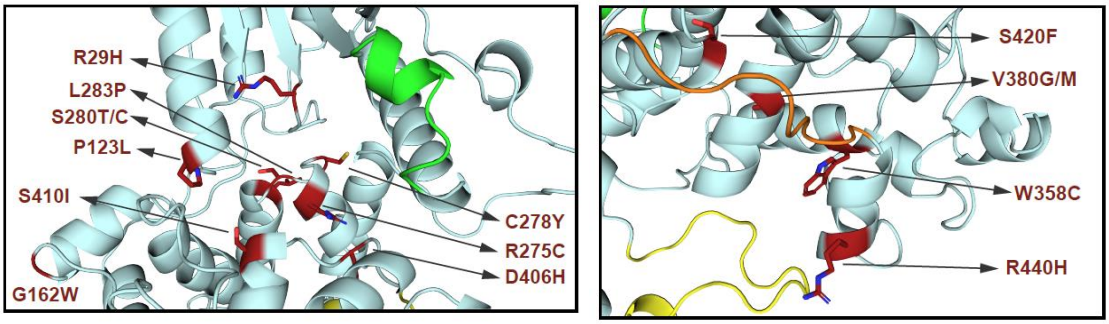

Figure 4.1. Visualization of SNPs on the mouse CRY2. The CRY2 variant residues (red) were visualized on mCRY2 as a ribbon diagram. The serine loop was colored green, and the P-loop yellow.

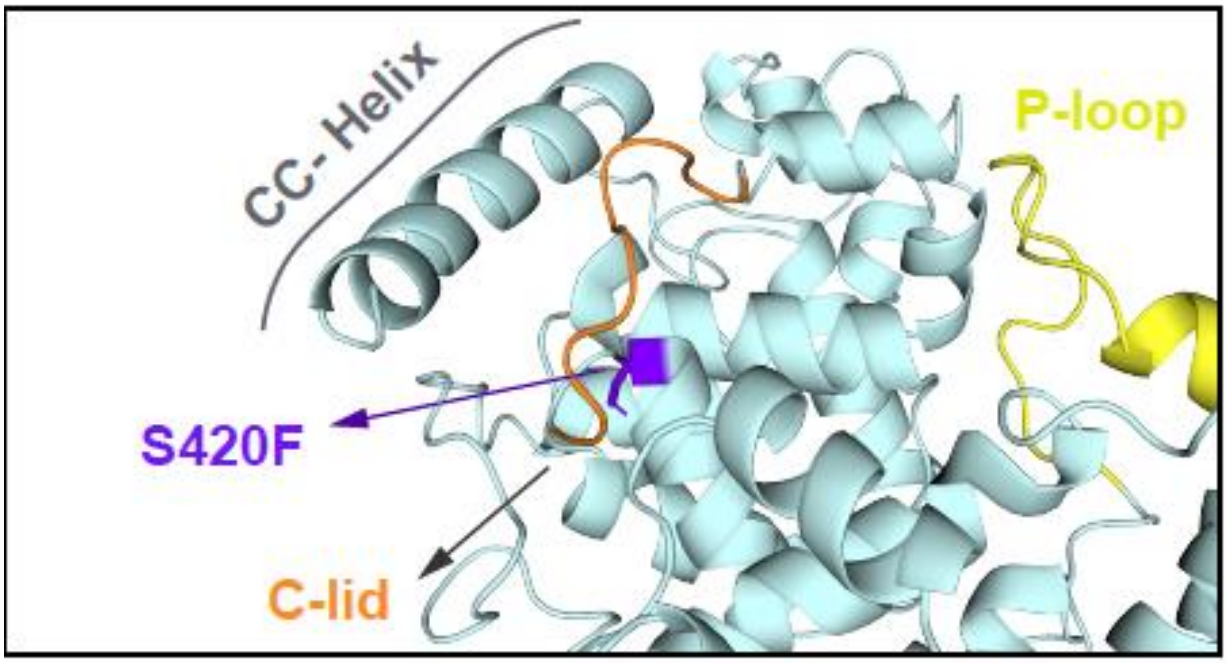

Figure 4.2. Visualization of p.Ser420Phe on the mouse CRY2. Ser420 residue (purple) was visualized on mCRY2 as a ribbon diagram. The C-lid was colored orange, and the P-loop yellow.

4.2. Per1-dLuc Repression assay of CLOCK–BMAL1–dependent transactivation

The Ser were replaced with Phe in CRY2 at the position of 420 using site-directed mutagenesis. After confirming the changes by sequencing, I tested its effect on the

repression activity on CLOCK-BMAL1-driven transcription is investigated with the *Per1*-dLuc, -Per1 promotor fused with a destabilized luciferase gene, assay in a dose-dependent manner using HEK 293T cell line. Expectedly, as the amount of plasmid containing WT CRY2 cDNA increased, luciferase activity decreased in a dose-dependent manner, which suggested that WT CRY2 represses CLOCK-BMAL1 transactivation *(Fig. 4.3.A)*. However, the luciferase activity was not decreased in a dose-dependent manner in the presence of Cry2 variant plasmid (of p.Ser420Phe CRY), which indicates that the variant could not repress CLOCK-BMAL1 transactivation *(Fig. 4.3.A)*. To understand if this difference between WT and CRY2 variant stem from the less protein expression, the expression of the proteins at different doses were investigated, and observed that the variant had reduced protein expression compared to WT at high doses (20 and 50 ng) *(Fig. 4.3.A)*. This suggested that CRY2 variants were less stable compared to WT CRY2. It is known that PER2 is required for the stability CRYs. I investigated that the stability of CRY2 might be rescued in the presence of PER2. Therefore, I performed a *Per1-dLuc* assay in the presence of the PER using a plasmid that encodes PER2 cDNA.

Although PER2 was able to rescue the stability of the CRY2 variant as assessed by Western blot *(Fig. 4.3.B)*, the CRY variant was unable to repress CLOCK-BMAL1 transactivation at the dose of 20 and 50 ng CRY2 plasmid variant *(Fig. 4.3.B)*. These results suggested that the CRY2 variant might have altered affinity to core clock proteins and, in turn, reduced repressor activity.

A

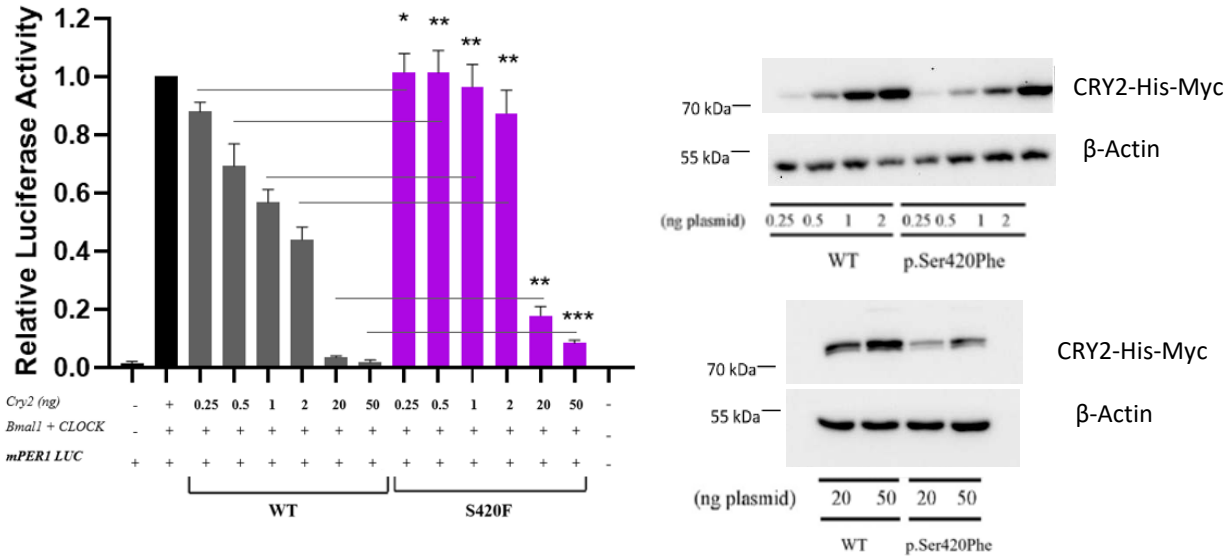

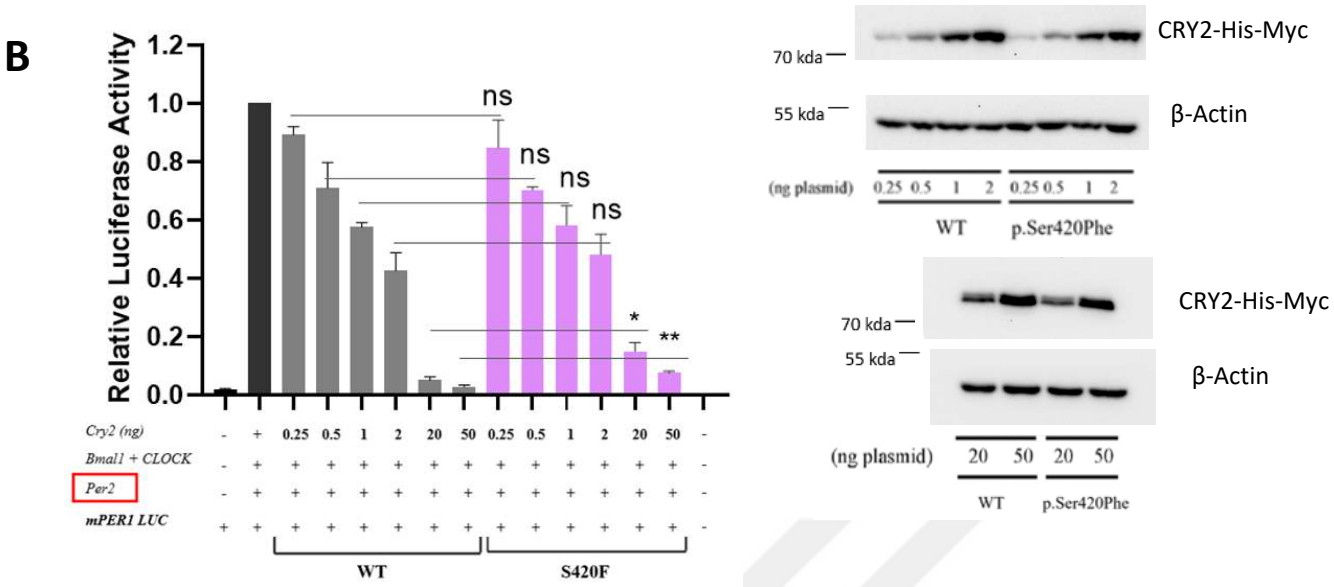

Figure 4.3. p.Ser420Phe CRY2 is loss-of-function variant. A, dose-dependent repression on CLOCK–BMAL1 transactivation of WT and p.Ser420Phe CRY2 in the absence and B, the presence of PER2 (n=3). HEK293T cells were transfected with 0.25 ng, 0.5 ng, 1 ng, 2 ng, 20 ng, and 50 ng of plasmids of WT or p.Ser420Phe CRY2. The data represent the mean of three biological replicates with at least three technical replicates. The equal dose of WT and mutant CRY2 was compared, and t-test was used for significance analysis (*p<0.05; **p<0.01; ***p<0.0005). The expression of each dose was controlled by Western blot. CRY2, cryptochrome 2; HEK293T, human embryonic kidney 293T cell line; PER2, period 2; WT, wild type.

4.3. Determination of the interaction between p.Ser420Phe CRY2 with CLOCK, BMAL1, and PER2

Since p.Ser420Phe CRY2 is located at the PHR domain, which is the region responsible for binding to the other core clock proteins (CLOCK, BMAL1, and PER2), the effect of the variant on the interaction was investigated with Co-IP. HEK293T cells were transfected with WT or variant pcDNA-*Cry2*-His-Myc plasmids, Flag-CMV-*CLOCK*, and Flag-CMV-*Bmal1*, with or without pFLAG-CMV-*PER2* overexpression. MYC resin was used to pull down pcDNA-*Cry2*-His-Myc, and the amounts of its binding partners Flag-CMV-*CLOCK*, Flag-CMV-*Bmal1*, and pFLAG-CMV-*PER2* were determined with Western blot. Analyses of the results showed that the affinity of p.Ser420Phe CRY2 to PER2 was reduced compared to WT, indicating that this region is important for CRY2-PER2 binding *(Fig. 4.4.A)*. Additionally, the interaction between

p.Ser420Phe CRY2 and CLOCK was also diminished in the absence of PER2; however, its affinity was rescued in the presence of PER2 *(Fig. 4.4.A, B)*. Moreover, the affinity of p.Ser420Phe CRY2 to BMAL1 did not significantly change in the absence and presence of PER2 *(Fig. 4.4.A, B)*. Further, co-IP experiments were performed between CRY2 variant and PER2 and CLOCK exclusively to get an understanding of how CRY2 variant alters the interaction with PER2 and CLOCK. These experiments reveal there is no significant change in the binding of the variant to the PER2 or CLOCK, unlike it is in the complex *(Fig. 4.4.C, D)*.

Co-IP experiments show that the variant exhibited comparable affinity to the CLOCK-BMAL1 complex in overexpressed PER2, which cannot explain the reduced repression activity. We, therefore, reasoned that variations' lower repressor activity might stem from improper nuclear localization.

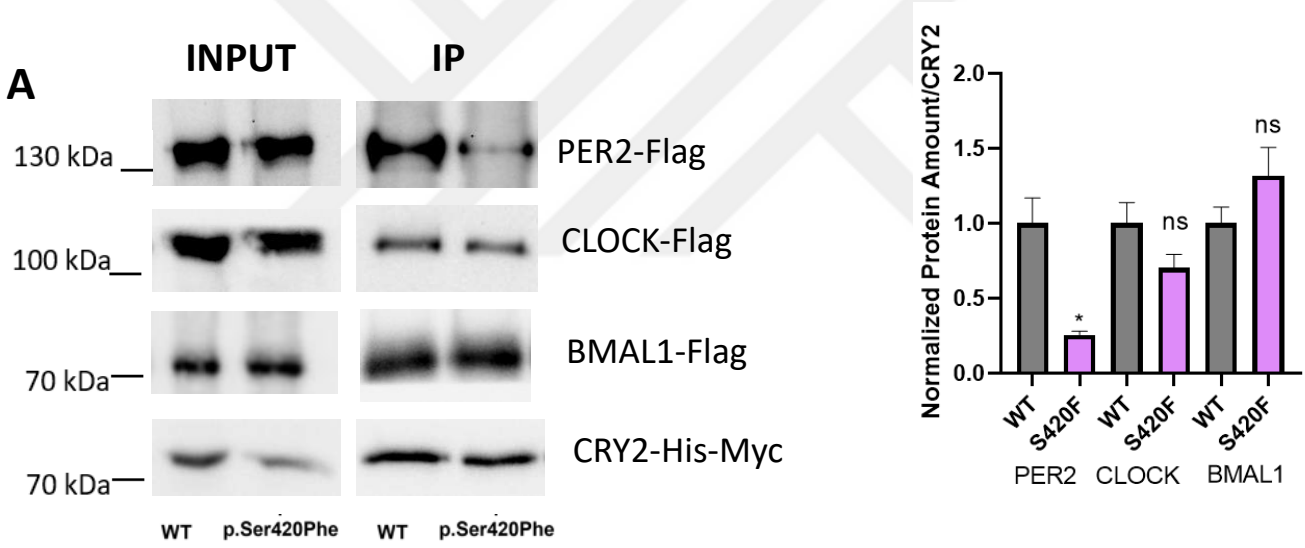

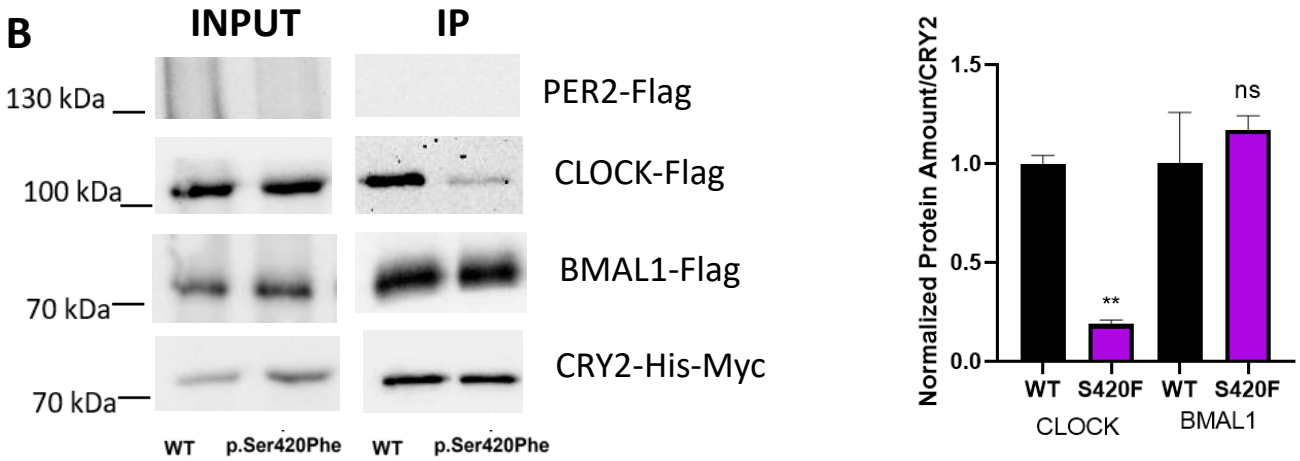

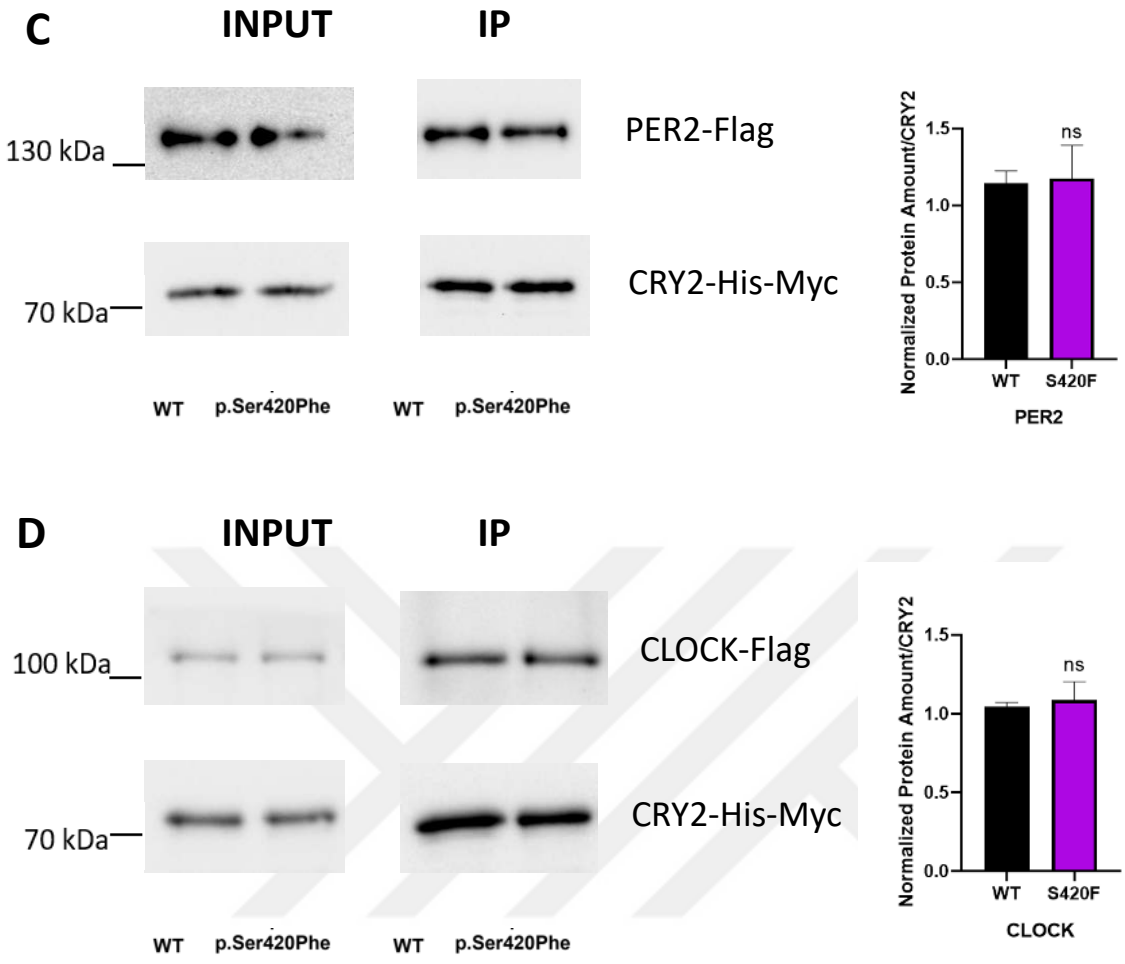

Figure 4.4. Determination of the interaction between p.Ser420Phe CRY2 with CLOCK, BMAL1, and PER2. A, physical interaction of WT and p.Ser420Phe CRY2 in the presence and B, the absence of PER2 (n=3). HEK293T cells were transfected with 500 ng WT or variant pcDNA-*Cry2*-His-Myc plasmids, 150 ng Flag-CMV-*CLOCK*, 1000 ng Flag-CMV-*Bmal1*, and 350 ng pFLAG-CMV-*PER2*. The next day, the cells were harvested, and Co-IP was performed using MYC resin. The amount of PER2, CLOCK, and BMAL1 was determined by Western blot and divided by the amount of CRY2, normalized based on WT. C, physical interaction of WT and p.Ser420Phe CRY2 with Flag-CMV-*CLOCK*. D, physical interaction of WT and p.Ser420Phe CRY2 with pFLAG-CMV-*PER2*. The unpaired t-test was used to determine significance (*p<0.05; **p<0.01). CRY2, cryptochrome 2; Co-IP, Co-Immunoprecipitation; HEK293T, human embryonic kidney 293T cell line; PER2, period 2; WT, wild type.

4.4. Subcellular Localization of p.Ser420Phe CRY2

Since the CC helix is also critical for nuclear shuttling, how the variant affects nuclear localization was investigated. Subcellular fractionation was performed to separate the nucleus and cytosol. To quantify the WT and variant CRY2 amount, Western blot was performed in the absence and presence of PER2. As a result of this experiment, it was observed that the cytosolic and nuclear level of the p.Ser420Phe CRY2 was significantly lower than that of the WT CRY2 in the absence of PER2, which implies the lower stability of the variant *(Fig. 4.5.B)*. Furthermore, the amounts of the variants in the nuclear fraction were considerably lower than WT even when PER2 is overexpressed, and this can explain why the CRY2 variant was not able to repress CLOCK–BMAL1–driven transcription even when PER2 is overexpressed.

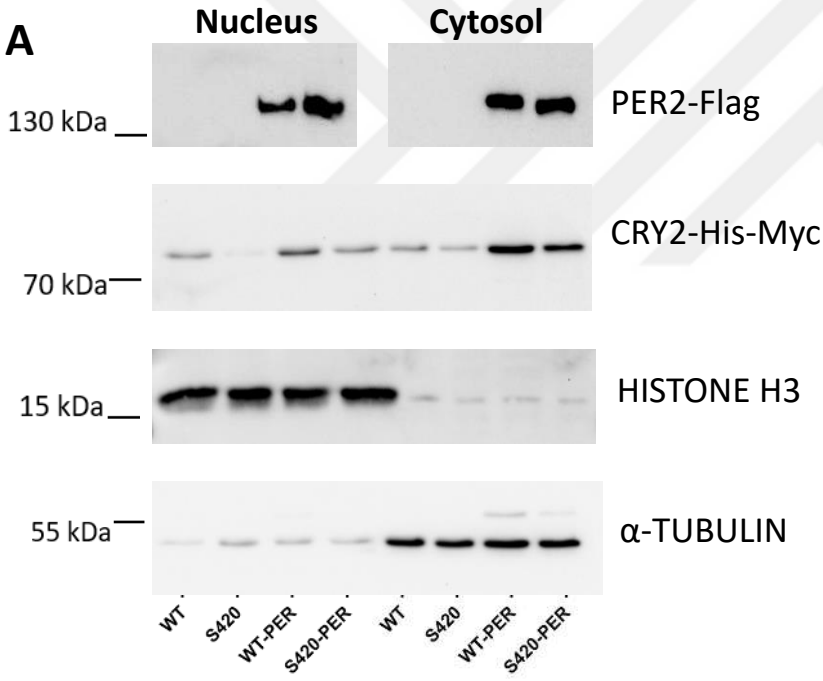

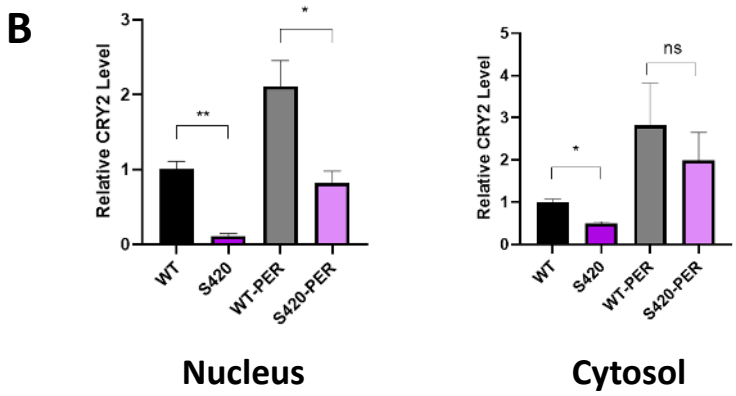

Figure 4.5. Subcellular localization of the WT and p.Ser420Phe CRY2. A, representative Western blot images of nuclear and cytosolic fractions of WT and p.Ser420Phe CRY2 in the absence and presence of PER2. Transfections of HEK293T cells with 500 ng WT or variant pcDNA-*Cry2*-His-Myc plasmids and 500 ng pFLAG-CMV-*PER2* were performed. The cells were extracted the following day, and subcellular fractionation was conducted. A, representative Western blot images of nuclear and cytosolic fractions of WT and p.Ser420Phe CRY2 in the absence and presence of PER2. Anti-Myc was used to detect the WT and variant CRY2. Alpha-tubulin and histone H3 were used as control. The amount of CRY2 was divided by histone H3 for nucleus and alpha-tubulin for cytosol and normalized based on WT. B, quantification of nuclear (left) and cytosolic (right) fractions of WT and p.Ser420Phe CRY2 in the absence and presence of PER2 ($n \geq 3$). The unpaired t-test was used for significance analysis (*$p<0.05$; **$p<0.01$). Separate comparisons were made between WT CRY2 and the variant. CRY2, cryptochrome 2; HEK293T, human embryonic kidney 293T cell line; PER2, period 2; WT, wild type.

4.5. Investigation of the Stability of p.Ser420Phe CRY2

As was observed in the subcellular fractionation, the amount of p.Ser420Phe CRY2 is lower than WT CRY2 in both the nucleus and cytosol, which implies that the variant may be less stable. And to investigate the stability, cycloheximide (CHX) chase experiments were performed. HEK293T cells were transfected with WT or variant pcDNA-*Cry2*-His-Myc. The following day, the cells were treated with CHX to inhibit protein synthesis and then harvested in 4-hour intervals for 12 hours. The CRY2 amounts were determined by Western blot, and compared to the WT, p.Ser420Phe was less stable and had a reduced half-life *(Fig. 4.6.A)*. The experiment was repeated by also overexpressing PER2, and the half-life of the variant became comparable to the WT *(Fig. 4.6.B)*.

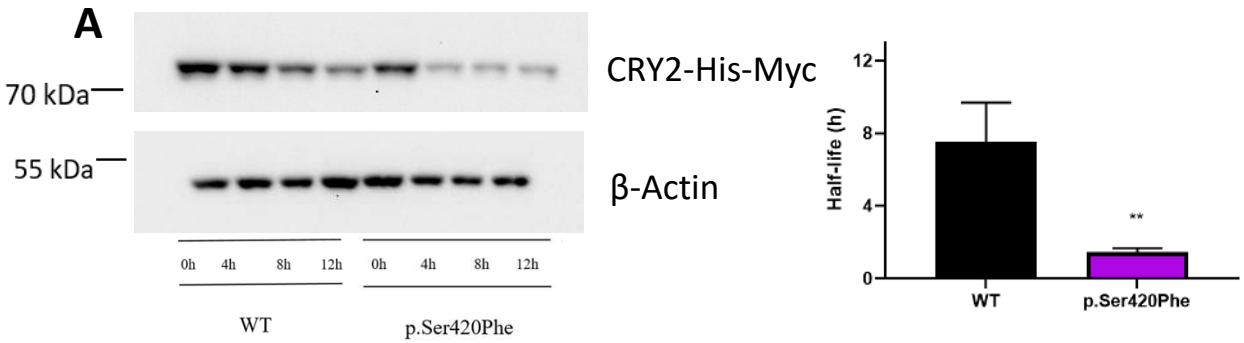

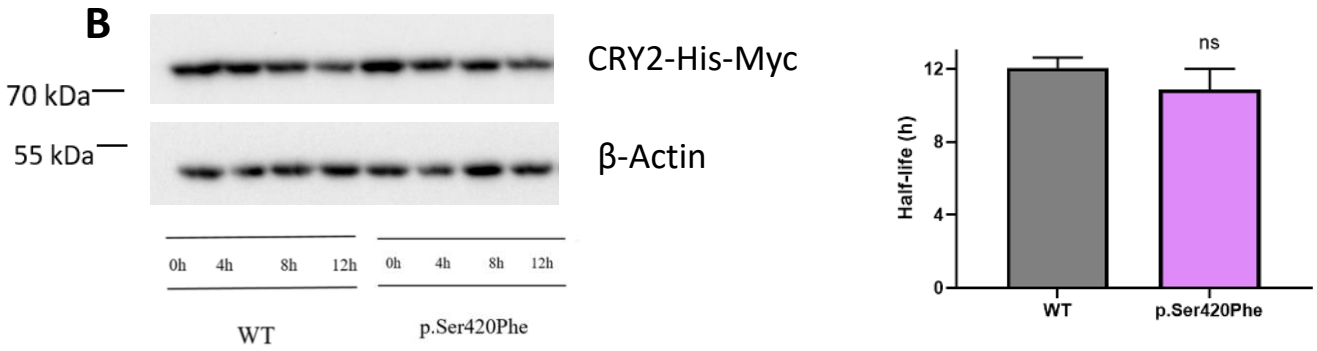

Figure 4.6. p.Ser420Phe CRY2 is less stable than WT CRY2. A, representative Western blot images of protein degradation assay of WT and p.Ser420Phe CRY2 in the absence and B, the presence of PER2 (n=3). HEK293T cells were transfected with 500 ng WT or mutant pcDNA-*Cry2*-His-Myc plasmids, as well as 500 ng pFLAG-CMV-*PER2*. The next day, the cells were treated with 20 μg/ml CHX to inhibit protein synthesis. The WT and variant CRY2 were detected with anti-Myc, and β-actin was used as a loading control. The half-lives of WT and p.Ser420Phe CRY2 were calculated using a one-phase exponential decay function with R^2 >0.95. The unpaired t-test was employed to test for significance (**p<0.01). CHX, cycloheximide; CRY2, cryptochrome 2; h, hour; HEK293T, human embryonic kidney 293T cell line; PER2, period 2; WT, wild type.

4.6. Proteasomal Degradation of p.Ser420Phe CRY2

Since CRYs degradation is mostly degraded by ubiquitin ligases, the CHX chase experiment with protease inhibitor MG132 treatment was used to study how the stability of the SNP is regulated. The Western blot results showed that inhibiting the proteasome resulted in the stabilization of WT CRY2 but not p.Ser420Phe CRY2, implying that p.Ser420Phe CRY2 was degraded by a noncanonical mechanism *(Fig. 4.7.B)*.

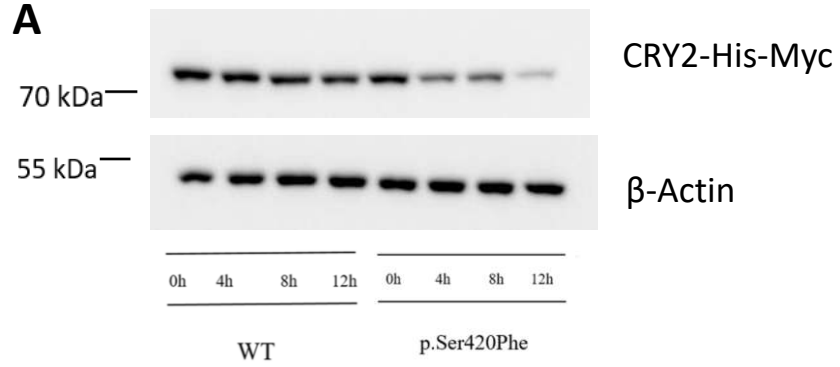

B

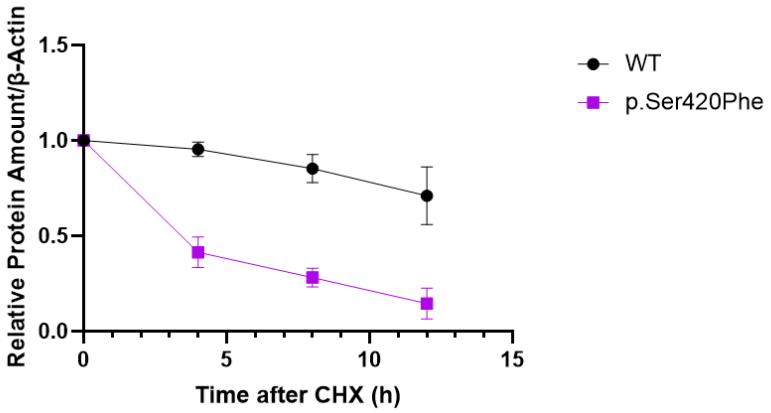

Figure 4.7. The stability of p.Ser420Phe CRY2 is not regulated by the proteasome. A, representative Western blot image of CHX chase assay of WT p.Ser420Phe CRY2 with MG132, a proteasome inhibitor treatment. 500 ng WT or variant pcDNA-*Cry2*-His-Myc plasmids were transfected to HEK293T cells. After overnight incubation, the cells were treated with 20 μg/ml CHX to inhibit protein synthesis and 10 μM MG132 to stop the proteasome. The WT and variant CRY2 were detected with anti-Myc, and β-actin was used as a loading control. B, quantification of Western blots (n=3). The amount of CRY2 was divided by β-actin and normalized based on 0 h. CHX, cycloheximide; CRY2, cryptochrome 2; h, hour; HEK293T, human embryonic kidney 293T cell line; WT, wild type.

4.7. Determination of the interaction between p.Ser420Phe CRY2 with FBXL3 and FBXL21

To understand the reason why p.Ser420Phe CRY2 was not degraded by the proteasome; the interaction of p.Ser420Phe with FBXL3 and FBXL21 was further investigated since they are the prominent ubiquitin ligases responsible for the degradation of CRY2. HEK293T cells were transfected with WT or variant pcDNA-*Cry2*-His-Myc plasmids, pBind-*FBXL3*-Gal4, and pFLAG-CMV-*FBXL21*. MYC resin was used to precipitate Myc-tagged CRY2, and the amount of FBXL3 and FBXL21 interacted with CRY2 was quantified by Western blot. The blots showed that the interaction between p.Ser420Phe CRY2 with both ubiquitin ligases disappeared *(Fig. 4.8.A, B)*. This could explain why p.Ser420Phe CRY2 was not degraded by the proteasome.

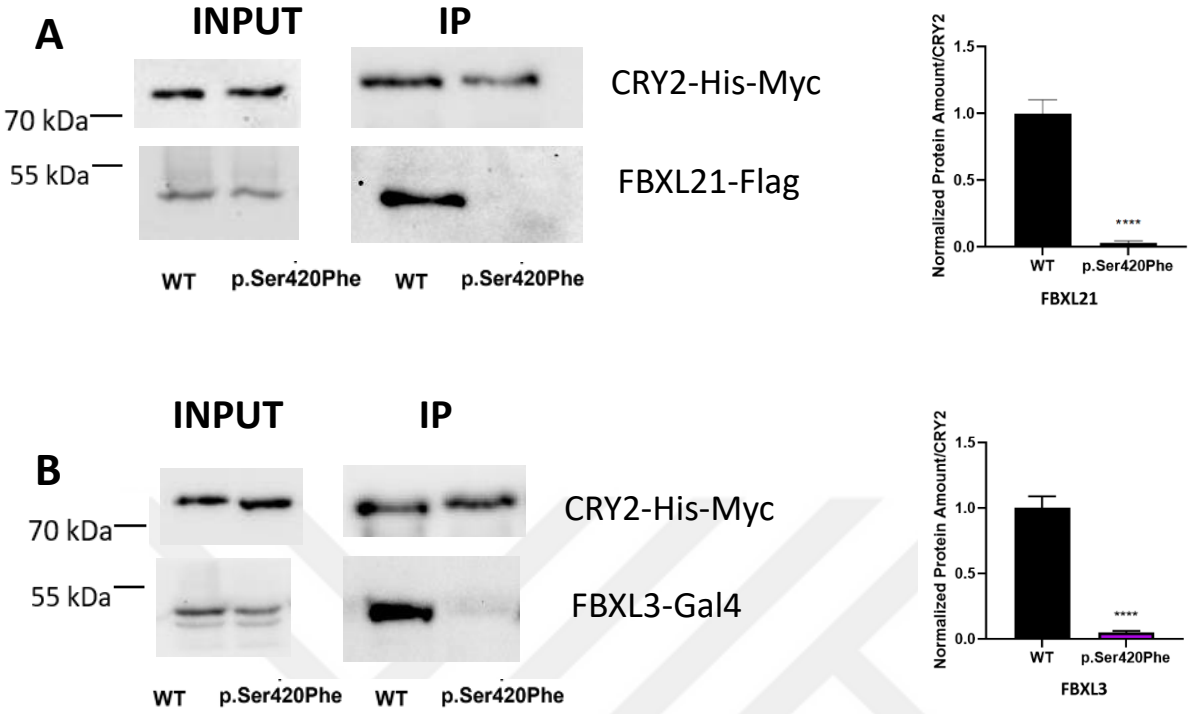

Figure 4.8. Determination of the interaction between p.Ser420Phe CRY2 with FBXL21 and FBXL3. A, the interaction between WT and p.Ser420Phe CRY2 with FBXL21 B, with FBXL3 (n≥3). HEK293T cells were transfected with 500 ng WT or variant pcDNA-*Cry2*-His-Myc plasmids, 500 ng pBind-*FBXL3*-Gal4, and 500 ng pFLAG-CMV-*FBXL21*. The cells were extracted the next day, and Co-IP was conducted with MYC resin. Western blot was used to quantify FBXL21 and FBXL3 and divided by the amount of CRY2, which was normalized based on WT. To evaluate the significance, the unpaired t-test was performed (****p<0.0001). CRY2, cryptochrome 2; Co-IP, Co-Immunoprecipitation; HEK293T, human embryonic kidney 293T cell line; WT, wild type.

4.8. Lysosomal Degradation of p.Ser420Phe CRY2

Previous study reveals that CRY1 is also degraded by the lysosomal pathway as an alternative to the proteasomal pathway (Toledo et al., 2018). Since it was concluded that p.Ser420Phe CRY2 was degraded by a noncanonical mechanism, thus, the lysosomal pathway was investigated by CHX chase assay with lysosome inhibitors PepstatinA and E64-d. SQSTM1 was used as an autophagy indicator; it was stabilized by the treatment of lysosome inhibitors, as expected, and degraded when the lysosome inhibitors were not added *(Fig. 4.9.A, C)*. The Western blot results showed that inhibiting the lysosome with

PepstatinA and E64-d increased the stability of both WT and p.Ser420Phe CRY2 *(Fig. 4.9.A)*. Therefore, it was concluded that p.Ser420Phe is degraded by lysosome.

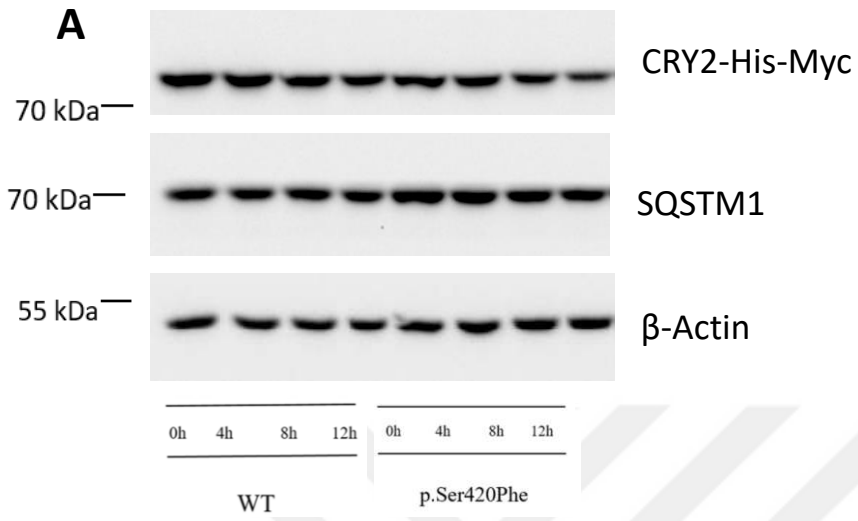

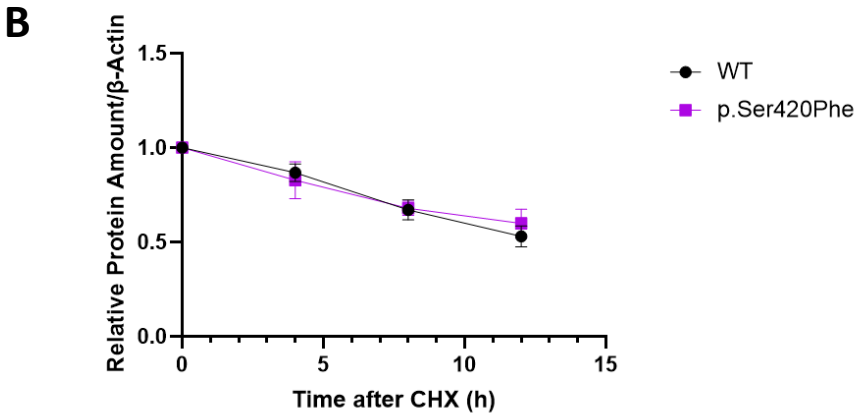

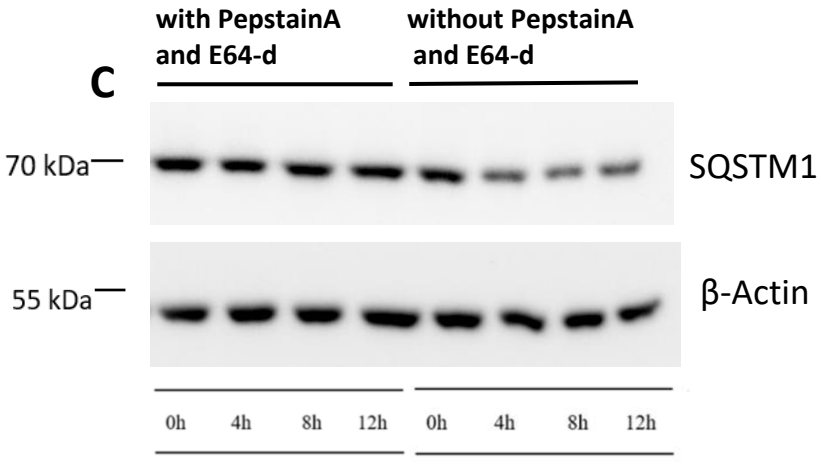

Figure 4.9. The stability of p.Ser420Phe CRY2 is regulated by the lysosome. A, representative Western blot image of CHX chase assay of WT p.Ser420Phe CRY2 with lysosome inhibitor treatment. 500 ng WT or variant pcDNA-*Cry2*-His-Myc plasmids were transfected to HEK293T cells. After overnight incubation, the cells were treated with 20 μg/ml CHX to inhibit protein synthesis and 5 μM PepstatinA and 5 μM E64-d to inhibit the lysosome. The WT and variant CRY2 were detected with anti-Myc, β-actin was used as a loading control, and SQSTM1 was used as an indicator of autophagic degradation. B, quantification of Western blots (n=3). The amount of CRY2 was divided by β-actin and normalized based on 0 h. C, Western blot image of CHX chase assay of SQSTM1 with and without treating lysosome inhibitors PepstatinA and E64-d. CHX, cycloheximide; CRY2, cryptochrome 2; h, hour; HEK293T, human embryonic kidney 293T cell line; WT, wild type.

4.9. The Effect of p.Ser420Phe CRY2 on circadian rhythm at the cellular level

Previous research suggests that CRY2 can restore the circadian rhythm in MEF *Cry1*$^{-/-}$*Cry2*$^{-/-}$ cells (Gul et al., 2020). Hence, a similar experiment was performed to examine the effect of CRY2 variation on the circadian rhythm compared to wild-type CRY2. For this purpose, MEF *Cry1*$^{-/-}$*Cry2*$^{-/-}$ cells were utilized because if only *Cry2*$^{-/-}$ cells were used, *Cry1* would compensate for the absence of *Cry2*, so the effect of the variant would not be evaluated. The cells were transfected with pMU2-P(*CRY1*)-(intron 336), WT or variant pMU2-P(*CRY1*)-(intron 336)-*Cry2*. pGL3-*Per2*-dLuc as a luciferase reporter to measure the bioluminescence, hence monitoring the circadian rhythm. Cells expressing WT *Cry1* and *Cry2* restored the circadian rhythm, as expected *(Fig. 4.10.)*. The p.Ser420Phe CRY2 rescued the rhythm to a certain degree, although with a significantly shorter period than WT, indicating reduced repression activity on CLOCK–BMAL1–dependent transactivation *(Fig. 4.10.)*.

A

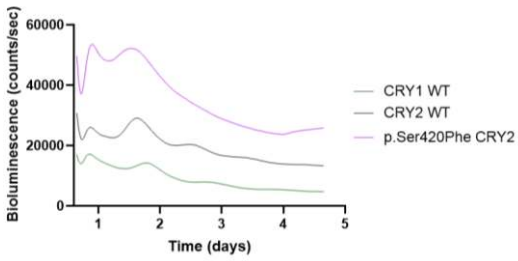

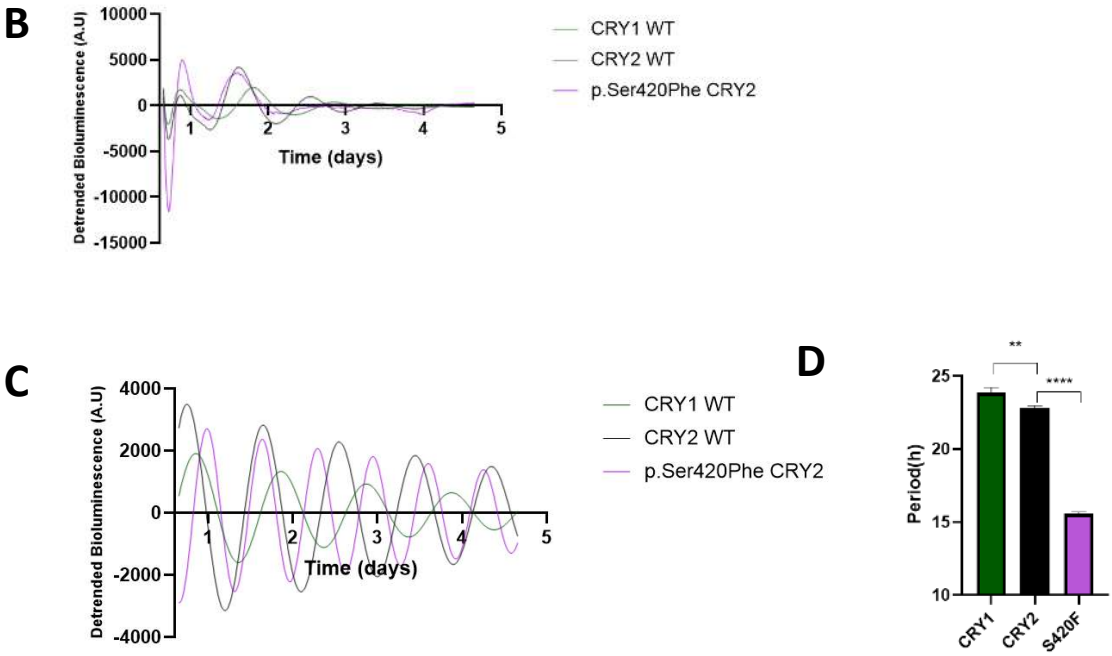

Figure 4.10. Real-Time bioluminescence rescue assay. A, the representative bioluminescence of WT CRY1, WT and p.Ser420Phe CRY2 (n=3). MEF *Cry1*$^{-/-}$*Cry2*$^{-/-}$ cells were transfected with WT CRY1 and WT and p.Ser420Phe CRY2 in pMU2 rescue plasmid. After 72 hours, the cells were synchronized with 0.1 μM DXM and the bioluminescence was recorded for 5 days. B, raw data were detrended by baseline-subtracting a 24-hour running average and, C, fitted to a sine wave using Lumicycle analysis software (Actimetrics) to determine the periods, D, the unpaired t-test was employed to test for the significance of the periods (**p<0.01; ****p<0.0001). CRY, cryptochrome; MEF, mouse embryonic fibroblast.

Chapter 5:
DISCUSSION

The circadian rhythm is a fundamental timing system that allows organisms to adapt to environmental changes and ensures their survival. It is regulated by interlocking transcriptional/translational feedback loops (TTFLs) at the molecular level, which involve interactions between core clock proteins (Kavakli et al., 2017; Kavakli et al., 2022a; Kavakli et al., 2022b). In the positive arm of the TTFL, the proteins CLOCK and BMAL1 form a heterodimer and initiate the transcription of clock-controlled genes by binding to the E-box element within the promoter region. On the other hand, in the negative arm of the TTFL, the proteins PERs (Periods) and CRYs (Cryptochromes), along with Casein kinase I, form a trimeric structure. Trimeric complex translocates into the nucleus and represses the transcription driven by BMAL1 and CLOCK (Kavakli et al., 2022b; Kavakli & Sancar, 2002). Studies have suggested a link between single nucleotide polymorphisms (SNPs) in core clock genes and certain diseases (Baris et al., 2023). Indeed, studies have identified associations between mutations in the CRY2 gene and various disorders. These include advanced sleep phase, attention-deficit/hyperactivity disorder (ADHD), familial delayed sleep phase disorder, and depression (Hirano et al., 2016c; Lavebratt et al., 2010; Onat et al., 2020; Patke et al., 2017). For instance, a specific CRY2 single nucleotide polymorphism (SNP) called A260T has been linked to familial advanced sleep phase sleep disorder. This SNP increases the interaction between CRY2 and FBXL3, resulting in reduced stability of CRY2 (Hirano et al., 2016c). This SNP was identified in a family affected by the sleep disorder. In this study, I identified a CRY2 variant (p.Ser420Phe CRY2) from the 1000 genome databank and functionally characterized its effect at the cellular level. However, no disease was diagnosed to segregate with this variation. The reason why could be this SNP is rare. This study shows that this SNP has a significant impact on the function of CRY2. To gain more insight into its function, the pathogenicity of this SNP could be further investigated *in vivo* to evaluate its relationship with disorders.

Cryptochromes structurally have two distinct domains, which are the PHR domain and extended C-terminal domains (Kavakli et al., 2017; Parico & Partch, 2020). In mammals, these two domains play a crucial role in the interaction of cryptochromes with the core clock and other proteins (Cal-Kayitmazbatir et al., 2021; Parico & Partch, 2020).

The C-terminal domain is intrinsically disordered and modulates the function of the PHR domain of CRYs (Parico & Partch, 2020). For example, in CRY1Δ11, exon 11 from the C-terminal tail is deleted and has enhanced repressor activity (Patke et al., 2017). Further investigation has shown that exon 11 of CRY1 indeed regulates the affinity of CRY1 for the CLOCK/BMAL1 dimer, thereby affecting its repressor activity (Parico et al., 2020). PHR domains are further divided into two domains; α-helical and α/β domains. The coiled-coil (CC)-helix on the CRY PHR domain interacts directly with the BMAL1 transactivation domain (TAD) and PER2 (Ozber et al., 2010; Xu et al., 2015). This interaction is important for the regulation of circadian rhythms and the molecular clock system.

In this thesis, I functionally characterized the p.Ser420Phe CRY2 variant, located at the CC helix at the cellular level. The functional analysis reveals that the repressor activity of the p.Ser420Phe CRY2 variant is significantly reduced either in the presence or absence of PER2. Further studies attribute such difference to the reduced affinity of p.Ser420Phe CRY2 variant to CLOCK/BMAL1. This is possibly due to the CRY2 variant being unable to bind BMAL1 TAD and interact with the PHR region of CRY2. In fact, studies showed that the CC helix of CRY1 is important for the interaction of its PHR and BMAL1 TAD domains and, in turn, regulates their activity protein-protein interaction (Parico & Partch, 2020; Parico et al., 2020; Xu et al., 2015).

The stability of the variant was considerably different, where the variant was significantly less stable in the absence of the PER2. Initially, I thought such instability was a result of better interaction between CRY2 and FBXLs (E3 ligases). To explore such a possibility, I performed Co-IP between the CRY2 variant and FBXLs. Surprisingly, there was no interaction between the CRY2 variant and FBXL3. FBXL3 is an E3 ligase that ubiquitinates CRYs and targets them for proteasomal degradation (Busino et al., 2007; Godinho et al., 2007; Xing et al., 2013). Although the CHX chase experiments show that the variant has reduced stability, it is rescued in the presence of PER2, which is in line with the expression of the variant. The affinity of the variant is reduced to PER2 when it is immunoprecipitated as a complex with BMAL1 and CLOCK, which cannot explain how the stability of the variant increases when PER2 is overexpressed. This could be explained by the results showing that the affinity to PER2 does not change when only PER2 is precipitated with CRY2. In addition, co-IP results show that the affinity of the variant to CLOCK also decreases. This variant shows that reduced affinity to PER2,

CLOCK, and FBXLs can stem from changes in the flexibility of the coiled-coil and possible conformational changes of CRY2, which needs to be investigated further with *in vitro* studies.

In my previous study, I showed that the SNPs at the rim of the secondary pockets could not properly localize to the nucleus, thus, showing reduced repressor activity (Parlak et al., 2022). In order to understand the reason why S420F CRY2 SNP has impaired repression on CLOCK-BMAL1, the localization of the variant is assessed. S420F shows lower levels in the nucleus even though PER2 is overexpressed, which explains the reduction in repression activity. Further functional analysis of this variant reveals that the variant is not degraded by proteasome; this could stem from the destroyed interaction between the variant and FBXL3 and FBXL21, which are prominently responsible for CRYs degradation. The reason for this lost interaction may be confirmational of the protein changes in a way that the region where FBXLs bind may be blocked. Although there are other FBXLs that are candidates for CRYs, the CHX chase assay performed with proteasome inhibitor MG132 eliminates the possible degradation with other ubiquitin ligases, such as FBXW7 (Wu et al., 2021). As an alternative to the proteasome, CRY1 is also degraded by lysosomes (Toledo et al., 2018). Therefore, lysosomal degradation is investigated by CHX chase assay with lysosome inhibitors PepstatinA and E64-d, and the stability of the S420F CRY2 SNP increased. This indicates that the degradation of the variant is regulated by the alternative lysosomal pathway. Further, the rhythm is also observed in MEF *Cry1*−/−*Cry2*−/− upon the expression of the variant CRY2, which also implies that the lysosomal degradation is important for the degradation because if the variant could not be degraded, there would not be a rhythm. It is shown that lysosomal degradation is also employed in CRY2, not just CRY1, which is a novel finding that fulfills this gap in the literature.

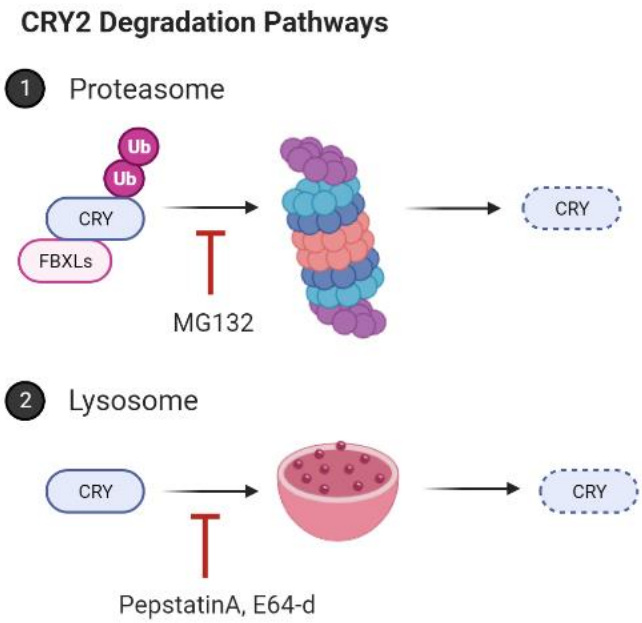

Figure 5.1. The depiction of CRY2 degradation pathways. CRY2 is degraded by 2 alternative pathways: proteasomal and lysosomal. MG132 inhibits proteasomal degradation. PepstatinA and E64-d inhibit lysosomal degradation.

BIBLIOGRAPHY

Aschoff, J., & Pohl, H. (1978). Phase relations between a circadian rhythm and its zeitgeber within the range of entrainment. *Naturwissenschaften, 65*, 80-84. Doi: 10.1007/BF00440545

Aschoff, J. (1979). Circadian rhythms: influences of internal and external factors on the period measured in constant conditions 1. *Zeitschrift für Tierpsychologie, 49*(3), 225-249. Doi: 10.1111/j.1439-0310.1979.tb00290.x

Aschoff, J. (1981). *A survey on biological rhythms* (pp. 3-10). Springer US. Doi: 10.1007/978-1-4615-6552-9_1

Balsalobre, A., Damiola, F., & Schibler, U. (1998). A serum shock induces circadian gene expression in mammalian tissue culture cells. *Cell, 93*(6), 929-937. Doi: 10.1016/S0092-8674(00)81199-X

Baris, I., Ozcan, O., & Kavakli, I. H. (2023). Single nucleotide polymorphisms (SNPs) in circadian genes: Impact on gene function and phenotype.

Busino, L., Bassermann, F., Maiolica, A., Lee, C., Nolan, P. M., Godinho, S. I., ... & Pagano, M. (2007). SCFFbxl3 controls the oscillation of the circadian clock by directing the degradation of cryptochrome proteins. *science*, 316(5826), 900-904. Doi: 10.1126/science.1141194

Cal-Kayitmazbatir, S., Kulkoyluoglu-Cotul, E., Growe, J., Selby, C. P., Rhoades, S. D., Malik, D., ... & Kavakli, I. H. (2021). CRY1-CBS binding regulates circadian clock function and metabolism. *The FEBS journal*, *288*(2), 614-639. Doi: 10.1111/febs.15360

Cao, X., Yang, Y., Selby, C. P., Liu, Z., & Sancar, A. (2021). Molecular mechanism of the repressive phase of the mammalian circadian clock. *Proceedings of the National Academy of Sciences, 118*(2), e2021174118. Doi: 10.1073/pnas.2021174118

Chaves, I., Yagita, K., Barnhoorn, S., Okamura, H., van der Horst, G. T., & Tamanini, F. (2006). Functional evolution of the photolyase/cryptochrome protein family: importance of the C terminus of mammalian CRY1 for circadian core oscillator performance. *Molecular and cellular biology*, *26*(5), 1743-1753. Doi: 10.1128/MCB.26.5.1743-1753.2006

Chen, Y., Hu, X., Liu, S., Su, T., Huang, H., Ren, H., ... & Lin, C. (2021). Regulation of Arabidopsis photoreceptor CRY2 by two distinct E3 ubiquitin ligases. *Nature communications, 12*(1), 2155. Doi: 10.1038/s41467-021-22410-x

Dhawka, L., Cha, Y., Ay, A., & Ingram, K. K. (2022). Low circadian amplitude and delayed phase are linked to seasonal affective disorder (SAD). *Journal of Affective Disorders Reports, 10*, 100395. Doi: 10.1016/j.jadr.2022.100395

Dibner, C., Schibler, U., & Albrecht, U. (2010). The mammalian circadian timing system: organization and coordination of central and peripheral clocks. *Annual review of physiology*, *72*, 517-549. Doi: 10.1146/annurev-physiol-021909-135821

Dunlap J.C., Loros J.J. & DeCoursey P.J. (2004). Chronobiology: Biological Timekeeping. Sinauer Associates. *Sunderland, MA*.

Evans, J., & Silver, R. (2022). The suprachiasmatic nucleus and the circadian timekeeping system of the body. In *Neuroscience in the 21st century: From basic to clinical* (pp. 2577-2625). Cham: Springer International Publishing. Doi: 10.1007/978-3-030-88832-9_66

Feng, D., & Lazar, M. A. (2012). Clocks, metabolism, and the epigenome. *Molecular cell, 47*(2), 158-167. Doi: 10.1016/j.molcel.2012.06.026

Fourier, C., Ran, C., Sjöstrand, C., Waldenlind, E., Steinberg, A., & Belin, A. C. (2021). The molecular clock gene cryptochrome 1 (CRY1) and its role in cluster headache. *Cephalalgia*, *41*(13), 1374-1381. Doi: 10.1177/03331024211024165

Fribourgh, J. L., Srivastava, A., Sandate, C. R., Michael, A. K., Hsu, P. L., Rakers, C., ... & Partch, C. L. (2020). Dynamics at the serine loop underlie differential affinity of cryptochromes for CLOCK: BMAL1 to control circadian timing. *Elife*, *9*, e55275. Doi: 10.7554/eLife.55275

Gao, P., Yoo, S. H., Lee, K. J., Rosensweig, C., Takahashi, J. S., Chen, B. P., & Green, C. B. (2013). Phosphorylation of the cryptochrome 1 C-terminal tail regulates circadian period length. *J Biol Chem, 288*(49), 35277-35286. Doi: 10.1074/jbc.M113.509604

Godinho, S. I., Maywood, E. S., Shaw, L., Tucci, V., Barnard, A. R., Busino, L., ... & Nolan, P. M. (2007). The after-hours mutant reveals a role for Fbxl3 in determining mammalian circadian period. *Science*, *316*(5826), 897-900. Doi: 10.1126/science.1141138

Goldman, B. D. (2001). Mammalian photoperiodic system: formal properties and neuroendocrine mechanisms of photoperiodic time measurement. *Journal of biological rhythms*, *16*(4), 283-301. Doi: 10.1177/074873001129001980

Gul, S., Aydin, C., Ozcan, O., Gurkan, B., Surme, S., Baris, I., & Kavakli, I. H. (2020). The Arg-293 of Cryptochrome1 is responsible for the allosteric regulation of CLOCK-CRY1 binding in circadian rhythm. *J Biol Chem, 295*(50), 17187-17199. doi:10.1074/jbc.RA120.014333

Hirano, A., Yumimoto, K., Tsunematsu, R., Matsumoto, M., Oyama, M., Kozuka-Hata, H., ... & Fukada, Y. (2013). FBXL21 regulates oscillation of the circadian clock through ubiquitination and stabilization of cryptochromes. *Cell, 152*(5), 1106-1118. Doi: 10.1016/j.cell.2013.01.054

Hirano, A., Nakagawa, T., Yoshitane, H., Oyama, M., Kozuka-Hata, H., Lanjakornsiripan, D., & Fukada, Y. (2016). USP7 and TDP-43: pleiotropic regulation of cryptochrome protein stability paces the oscillation of the mammalian circadian clock. *PLoS One*, 11(4), e0154263 a. Doi: 10.1371/journal.pone.0154263

Hirano, A., Fu, Y. H., & Ptáček, L. J. (2016). The intricate dance of post-translational modifications in the rhythm of life. *Nature structural & molecular biology, 23*(12), 1053-1060 b. Doi: 10.1038/nsmb.3326

Hirano, A., Shi, G., Jones, C. R., Lipzen, A., Pennacchio, L. A., Xu, Y., . . . Fu, Y. H. (2016). A Cryptochrome 2 mutation yields advanced sleep phase in humans. *Elife, 5* c. Doi: 10.7554/eLife.16695

Hogenesch, J. B., Chan, W. K., Jackiw, V. H., Brown, R. C., Gu, Y. Z., Pray-Grant, M., ... & Bradfield, C. A. (1997). Characterization of a subset of the basic-helix-loop-helix-PAS superfamily that interacts with components of the dioxin signaling pathway. *Journal of Biological Chemistry, 272*(13), 8581-8593. Doi: 10.1074/jbc.272.13.8581

Hsu, D. S., Zhao, X., Zhao, S., Kazantsev, A., Wang, R. P., Todo, T., ... & Sancar, A. (1996). Putative human blue-light photoreceptors hCRY1 and hCRY2 are flavoproteins. *Biochemistry*, *35*(44), 13871-13877. Doi: 10.1021/bi962209o

Huang, N., Chelliah, Y., Shan, Y., Taylor, C. A., Yoo, S. H., Partch, C., ... & Takahashi, J. S. (2012). Crystal structure of the heterodimeric CLOCK: BMAL1 transcriptional activator complex. *Science*, *337*(6091), 189-194. Doi: 10.1126/science.1222804

Kavaklı, Í. H., & Sancar, A. (2002). Circadian photoreception in humans and mice. *Molecular Interventions, 2*(8), 484. Doi: 10.1124/mi.2.8.484

Kavakli, I. H., Baris, I., Tardu, M., Gül, Ş., Öner, H., Cal, S., ... & Aydın, C. (2017). The photolyase/cryptochrome family of proteins as DNA repair enzymes and transcriptional repressors. *Photochemistry and photobiology*, *93*(1), 93-103. Doi: 10.1111/php.12669

Kavakli, I. H., Gul, S., & Turkay, M. (2022). Identification of novel small molecules targeting core clock proteins to regulate circadian rhythm. *Current Opinion in Chemical Engineering*, *35*, 100730 a. Doi: 10.1016/j.coche.2021.100730

Kavakli, I. H., Ozturk, N., & Baris, I. (2022). Protein interaction networks of the mammalian core clock proteins. *Adv. Protein Chem. Struct. Biol*, *131*, 207-233 b.

Klarsfeld, A., & d'Ortous, J. J. (2013). At the dawn of chronobiology. *Translated by Helen Tomlin*.

Khan, S. K., Xu, H., Ukai-Tadenuma, M., Burton, B., Wang, Y., Ueda, H. R., & Liu, A. C. (2012). Identification of a novel cryptochrome differentiating domain required for feedback repression in circadian clock function. *J Biol Chem, 287*(31), 25917-25926. Doi: 10.1074/jbc.M112.368001

Ko, C. H., & Takahashi, J. S. (2006). Molecular components of the mammalian circadian clock. *Human molecular genetics, 15*(suppl_2), R271-R277. Doi: 10.1093/hmg/ddl207

Koike, N., Yoo, S. H., Huang, H. C., Kumar, V., Lee, C., Kim, T. K., & Takahashi, J. S. (2012). Transcriptional architecture and chromatin landscape of the core circadian clock in mammals. *science, 338*(6105), 349-354. Doi: 10.1126/science.1226339

Kovanen, L., Kaunisto, M., Donner, K., Saarikoski, S. T., & Partonen, T. (2013). CRY2 genetic variants associate with dysthymia. *PLoS One, 8*(8), e71450. Doi: 10.1371/ journal.pone.0071450

Lamia, K. A., Sachdeva, U. M., DiTacchio, L., Williams, E. C., Alvarez, J. G., Egan, D. F., ... & Evans, R. M. (2009). AMPK regulates the circadian clock by cryptochrome phosphorylation and degradation. *Science*, 326(5951), 437-440. Doi: 10.1126/science.1172156

Lavebratt, C., Sjöholm, L. K., Soronen, P., Paunio, T., Vawter, M. P., Bunney, W. E., ... & Schalling, M. (2010). CRY2 is associated with depression. *Plos one, 5*(2), e9407. Doi: 10.1371/journal.pone.0009407

Liu, C., Li, H., Qi, L., Loos, R. J., Qi, Q., Lu, L., ... & Lin, X. (2011). Variants in GLIS3 and CRY2 are associated with type 2 diabetes and impaired fasting glucose in Chinese Hans. *PLoS One*, *6*(6), e21464. Doi: 10.1371/journal.pone.0021464

Mohawk, J. A., Green, C. B., & Takahashi, J. S. (2012). Central and peripheral circadian clocks in mammals. *Annual review of neuroscience*, *35*, 445-462. Doi: 10.1146/annurev-neuro-060909-153128

Moore, R. Y., & Eichler, V. B. (1972). Loss of a circadian adrenal corticosterone rhythm following suprachiasmatic lesions in the rat. *Brain research. 42*(1), 201–206. Doi: 10.1016/0006-8993(72)90054-6

Nangle, S. N., Rosensweig, C., Koike, N., Tei, H., Takahashi, J. S., Green, C. B., & Zheng, N. (2014). Molecular assembly of the period-cryptochrome circadian transcriptional repressor complex. *Elife, 3*, e03674. Doi: 10.7554/eLife.03674

Onat, O. E., Kars, M. E., Gul, S., Bilguvar, K., Wu, Y., Ozhan, A., . . . Ozcelik, T. (2020). Human CRY1 variants associate with attention deficit/hyperactivity disorder. *J Clin Invest, 130*(7), 3885-3900. Doi:10.1172/JCI135500

Ozber, N., Baris, I., Tatlici, G., Gur, I., Kilinc, S., Unal, E. B., & Kavakli, I. H. (2010). Identification of two Amino Acids in the C-terminal Domain of Mouse CRY2 Essential for PER2 Interaction. *BMC Molecular Biology, 11*. Doi: 10.1186/1471-2199-11-69

Ozcan, O., Gul, S., & Kavakli, I. H. (2021). Allosteric regulation of CRYs in mammalian circadian clock. In *Computer Aided Chemical Engineering* (Vol. 50, pp. 2025-2031). Elsevier. Doi: 10.1016/B978-0-323-88506-5.50313-2

Ozturk, N. (2017). Phylogenetic and functional classification of the photolyase/cryptochrome family. *Photochemistry and photobiology*, *93*(1), 104-111. Doi: 10.1111/php.12676

Özgür, S., & Sancar, A. (2003). Purification and properties of human blue-light photoreceptor cryptochrome 2. *Biochemistry, 42(*10), 2926-2932. Doi: 10.1021/bi026963n

Parlak, G. C., Camur, B. B., Gul, S., Ozcan, O., Baris, I., & Kavakli, I. H. (2022). The secondary pocket of cryptochrome 2 is important for the regulation of its stability and localization. *Journal of Biological Chemistry*, *298*(9). Doi: 10.1016/j.jbc.2022.102334

Parico, G. C. G., & Partch, C. L. (2020). The tail of cryptochromes: an intrinsically disordered cog within the mammalian circadian clock. *Cell Communication and Signaling*, *18*, 1-9. Doi: 10.1186/s12964-020-00665-z

Patke, A., Murphy, P. J., Onat, O. E., Krieger, A. C., Özçelik, T., Campbell, S. S., & Young, M. W. (2017). Mutation of the human circadian clock gene CRY1 in familial delayed sleep phase disorder. *Cell*, *169*(2), 203-215. Doi: 10.1016/j.cell.2017.03.027

Pittendrigh, C. S. (1981). Circadian systems: entrainment. *Biological rhythms*, 95-124. Doi: 10.1007/BF01417859

Reischl, S., Vanselow, K., Westermark, P. O., Thierfelder, N., Maier, B., Herzel, H., & Kramer, A. (2007). β-TrCP1-mediated degradation of PERIOD2 is essential for circadian dynamics. *Journal of biological rhythms*, *22*(5), 375-386. Doi: 10.1177/0748730407303926

Ripperger, J. A., & Schibler, U. (2006). Rhythmic CLOCK-BMAL1 binding to multiple E-box motifs drives circadian Dbp transcription and chromatin transitions. *Nature genetics, 38*(3), 369-374. Doi: 10.1038/ng1738

Rutovskaya, M. V., Kosyreva, A. M., & Diatroptov, M. E. (2020). Ultradian and infradian rhythms in the dynamic of testosterone concentration in the serum of the white-breasted hedgehog Erinaceus roumanicus. *Scientific Reports, 10*(1), 6334. Doi: 10.1038/s41598-020-63399-5

Rosensweig, C., Reynolds, K. A., Gao, P., Laothamatas, I., Shan, Y., Ranganathan, R., ... & Green, C. B. (2018). An evolutionary hotspot defines functional differences between CRYPTOCHROMES. *Nature communications*, *9*(1), 1138. Doi: 10.1038/s41467-018-03503-6.

Salazar, P., Konda, S., Sridhar, A., Arbieva, Z., Daviglus, M., Darbar, D., & Rehman, J. (2021). Common genetic variation in circadian clock genes are associated with cardiovascular risk factors in an African American and Hispanic/Latino cohort. *IJC Heart & Vasculature, 34*, 100808. Doi: 10.1016/j.ijcha.2021.100808

Saini, R., Jaskolski, M., & Davis, S. J. (2019). Circadian oscillator proteins across the kingdoms of life: structural aspects. *BMC biology, 17*(1), 1-39. Doi: 10.1186/s12915-018-0623-3

Schmalen, I., Reischl, S., Wallach, T., Klemz, R., Grudziecki, A., Prabu, J. R., ... & Wolf, E. (2014). Interaction of circadian clock proteins CRY1 and PER2 is modulated

by zinc binding and disulfide bond formation. *Cell, 157*(5), 1203-1215. Doi: 10.1016/j.cell.2014.03.057

Siepka, S. M., Yoo, S. H., Park, J., Song, W., Kumar, V., Hu, Y., ... & Takahashi, J. S. (2007). Circadian mutant Overtime reveals F-box protein FBXL3 regulation of cryptochrome and period gene expression. *Cell, 129*(5), 1011-1023. Doi: 10.1016/j.cell.2007.04.030

Takahashi, J. S. (2017). Transcriptional architecture of the mammalian circadian clock. *Nature Reviews Genetics*, *18*(3), 164-179. Doi: 10.1038/nrg.2016.150

Toledo, M., Batista-Gonzalez, A., Merheb, E., Aoun, M. L., Tarabra, E., Feng, D., ... & Singh, R. (2018). Autophagy regulates the liver clock and glucose metabolism by degrading CRY1. *Cell metabolism*, 28(2), 268-281. Doi: 10.1016/j.cmet.2018.05.023

Vitaterna, M. H., King, D. P., Chang, A. M., Kornhauser, J. M., Lowrey, P. L., McDonald, J. D., ... & Takahashi, J. S. (1994). Mutagenesis and mapping of a mouse gene, Clock, essential for circadian behavior. *Science, 264*(5159), 719-725. Doi: 10.1126/science.8171325

Vitaterna, M. H., Takahashi, J. S., & Turek, F. W. (2001). Overview of circadian rhythms. *Alcohol research & health, 25*(2), 85.

Wang, H. (2018). Perfect timing: a Nobel Prize in Physiology or Medicine for circadian clocks. *Sci Bull, 63*(7), 398-401. Doi: 10.1016/j.scib.2018.02.009

Wu, L., Liu, Q., Fan, C., Yi, X., & Cheng, B. (2021). MALAT1 recruited the E3 ubiquitin ligase FBXW7 to induce CRY2 ubiquitin-mediated degradation and participated in trophoblast migration and invasion. *Journal of Cellular Physiology*, 236(3), 2169-2177. Doi: 10.1002/jcp.30003

Xing, W., Busino, L., Hinds, T. R., Marionni, S. T., Saifee, N. H., Bush, M. F., ... & Zheng, N. (2013). SCFFBXL3 ubiquitin ligase targets cryptochromes at their cofactor pocket. *Nature, 496*(7443), 64-68. Doi: doi.org/10.1038/nature11964

Xu, H., Gustafson, C. L., Sammons, P. J., Khan, S. K., Parsley, N. C., Ramanathan, C., ... & Partch, C. L. (2015). Cryptochrome 1 regulates the circadian clock through dynamic interactions with the BMAL1 C terminus. *Nature structural & molecular biology*, *22*(6), 476-484. Doi: 10.1038/nsmb.3018

Yoo, S. H., Mohawk, J. A., Siepka, S. M., Shan, Y., Huh, S. K., Hong, H. K., . . . Takahashi, J. S. (2013). Competing E3 ubiquitin ligases govern circadian periodicity by

degradation of CRY in nucleus and cytoplasm. *Cell, 152*(5), 1091-1105. Doi: 10.1016/j.cell.2013.01.055

Zuo, Z. C., Meng, Y. Y., Yu, X. H., Zhang, Z. L., Feng, D. S., Sun, S. F., ... & Lin, C. T. (2012). A study of the blue-light-dependent phosphorylation, degradation, and photobody formation of Arabidopsis CRY2. *Molecular plant, 5*(3), 726-733. Doi: 10.1093/mp/sss007

Appendix A: Supplementary Data

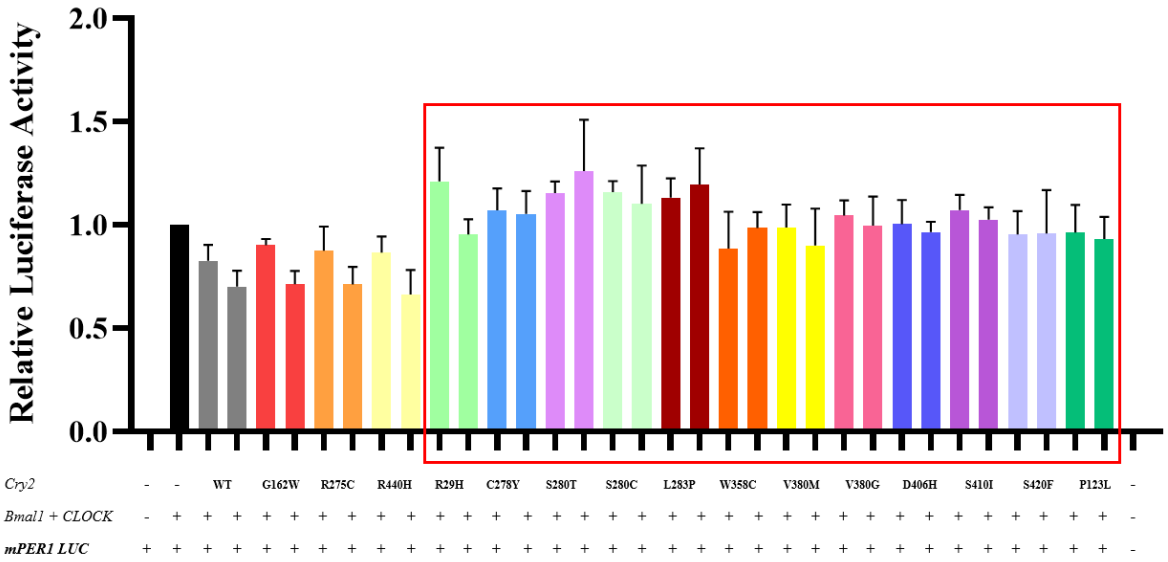

Figure A.1. Preliminary *Per1-dLuc* Repression assay on CLOCK–BMAL1 of WT and rare CRY2 SNPs. HEK293T cells were transfected with 0.25 ng and 0.5 ng of plasmids of WT or variant CRY2. The data represent the mean of three biological replicates with at least three technical replicates. CRY2, cryptochrome 2; HEK293T, human embryonic kidney 293T cell line; WT, wild type.

Appendix B: DNA and Protein Markers

GeneRuler 1 kb DNA Ladder

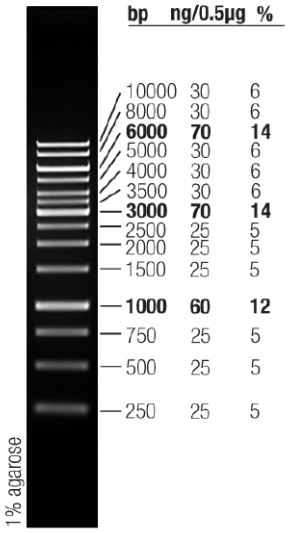

0.5 µg/lane, 8 cm length gel,
1X TAE, 7 V/cm, 45 min

PageRuler Prestained Protein Ladder

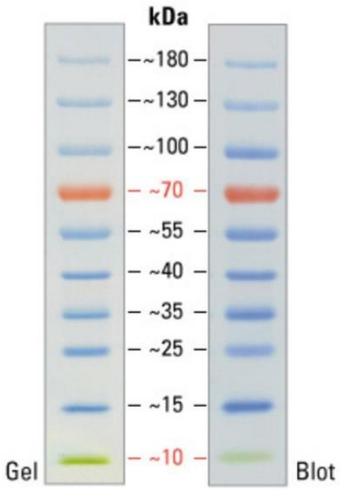

4-20% Tris-glycine SDS-PAGE

Appendix C: Expression Vector Maps

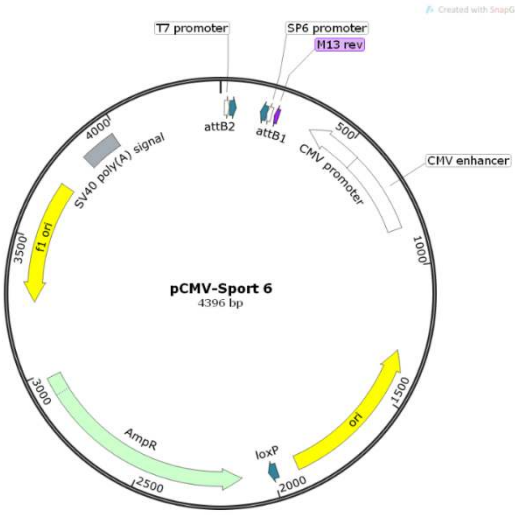

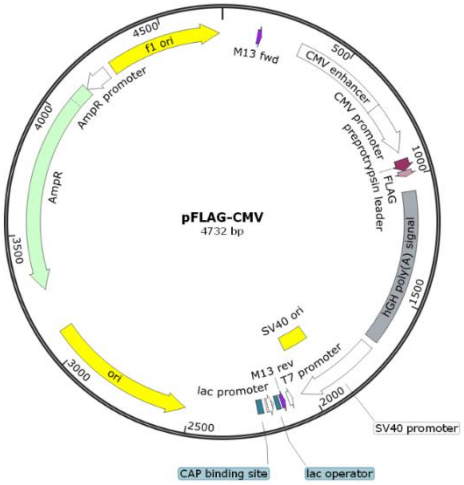

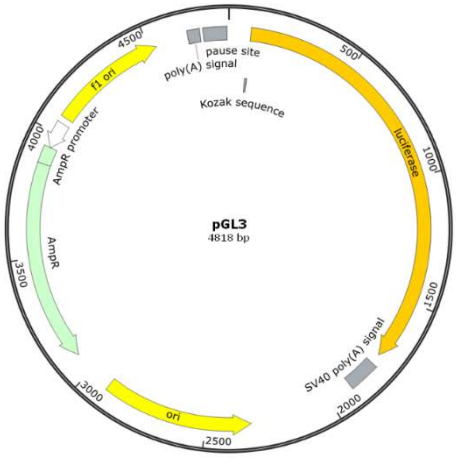

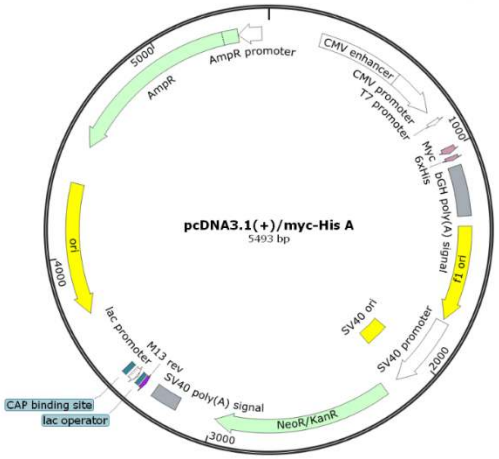

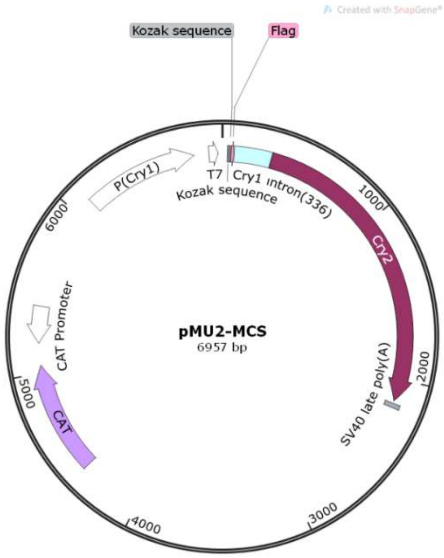

Appendix D: Rights and Permissions

25.05.2023 14:34 RightsLink Printable License

SPRINGER NATURE LICENSE
TERMS AND CONDITIONS

May 25, 2023

This Agreement between Koç University -- Gizem Çağla Parlak ("You") and Springer Nature ("Springer Nature") consists of your license details and the terms and conditions provided by Springer Nature and Copyright Clearance Center.

License Number	5555890630069
License date	May 25, 2023
Licensed Content Publisher	Springer Nature
Licensed Content Publication	Springer eBook
Licensed Content Title	The Suprachiasmatic Nucleus and the Circadian Timekeeping System of the Body
Licensed Content Author	Jennifer Evans, Rae Silver
Licensed Content Date	Jan 1, 2016
Type of Use	Thesis/Dissertation
Requestor type	academic/university or research institute
Format	print and electronic
Portion	figures/tables/illustrations
Number of figures/tables/illustrations	1

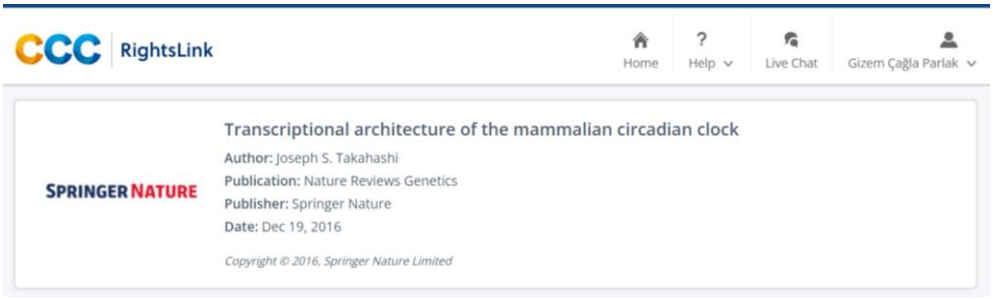

SPRINGER NATURE LICENSE
TERMS AND CONDITIONS

May 25, 2023

This Agreement between Koç University -- Gizem Çağla Parlak ("You") and Springer Nature ("Springer Nature") consists of your license details and the terms and conditions provided by Springer Nature and Copyright Clearance Center.

License Number	5555880132075
License date	May 25, 2023
Licensed Content Publisher	Springer Nature
Licensed Content Publication	Nature Reviews Genetics
Licensed Content Title	Transcriptional architecture of the mammalian circadian clock
Licensed Content Author	Joseph S. Takahashi
Licensed Content Date	Dec 19, 2016
Type of Use	Thesis/Dissertation
Requestor type	academic/university or research institute
Format	print and electronic
Portion	figures/tables/illustrations
Number of figures/tables/illustrations	1
Would you like a high resolution image with your order?	no
Will you be translating?	no